ERDC/CRREL SR-24-2

Cold Regions Research and Engineering Laboratory

U.S. ARMY

US Army Corps of Engineers®

ERDC

Porosity Measurement Device Design and Analysis

Cody M. Best, Carl R. Hart, and Christopher J. Donnelly

June 2024

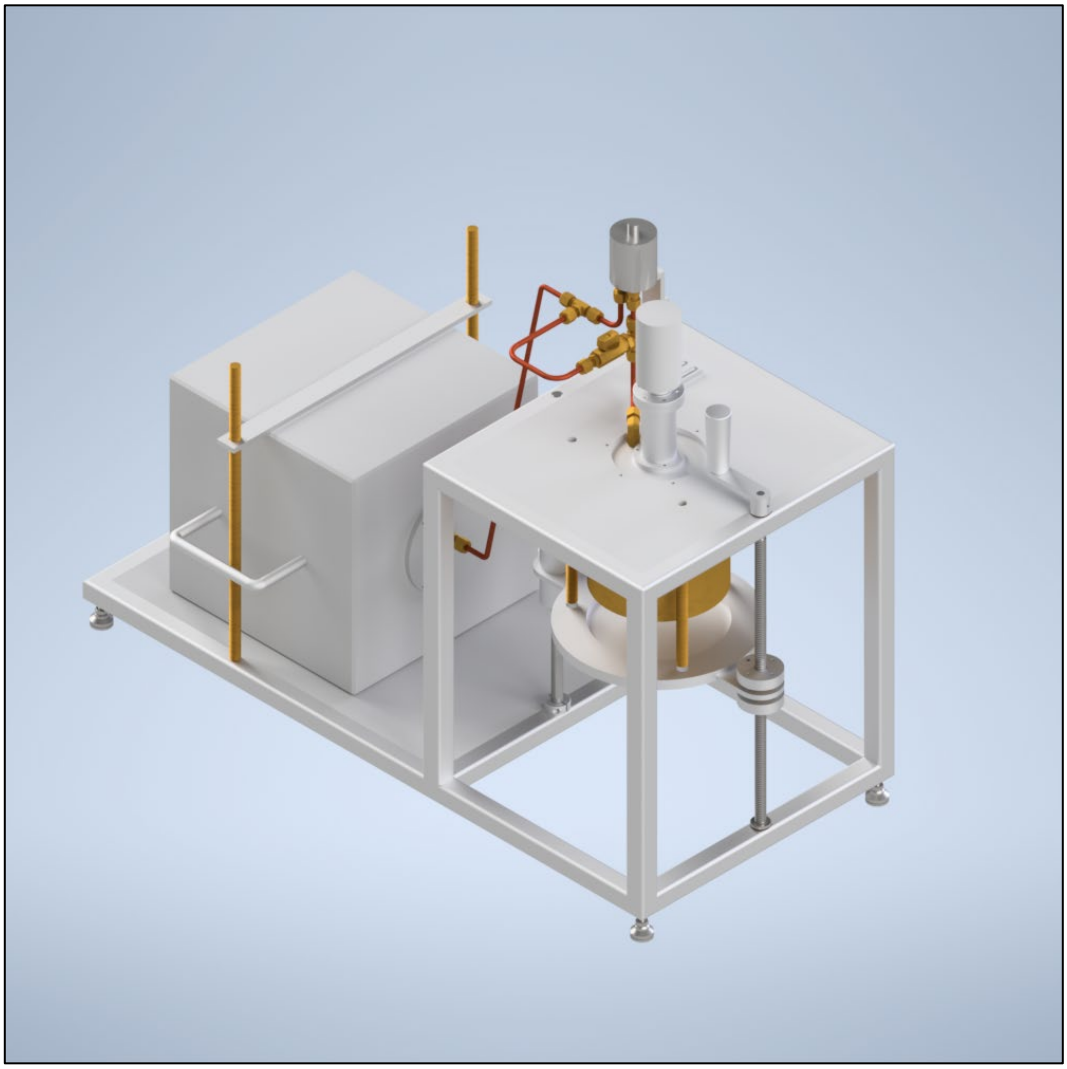

The US Army Engineer Research and Development Center (ERDC) solves the nation's toughest engineering and environmental challenges. ERDC develops innovative solutions in civil and military engineering, geospatial sciences, water resources, and environmental sciences for the Army, the Department of Defense, civilian agencies, and our nation's public good. Find out more at www.erdc.usace.army.mil.

To search for other technical reports published by ERDC, visit the ERDC online library at https://erdclibrary.on.worldcat.org/discovery.

ERDC/CRREL SR-24-2
June 2024

Porosity Measurement Device Design and Analysis

Cody M. Best, Carl R. Hart, and Christopher J. Donnelly

US Army Engineer Research and Development Center (ERDC)
Cold Regions Research and Engineering Laboratory (CRREL)
72 Lyme Road
Hanover, NH 03755-1290

Final Special Report (SR)

Prepared for US Army Corps of Engineers
Washington, DC 20314-1000

Under Program Element 601102A, Project Number AB2

Abstract

Porosity measurements are necessary to fully characterize the acoustic properties of a porous material. Many methods exist to measure porosity with various limitations. This report details a system based on previous work to limit environmental effects on measurements.

Contents

Figures and Tables

Figures

Tables

Preface

This study was conducted for the US Army Corps of Engineers (USACE) under Program Element 601102A, Project Number AB2, "Nonlinear Effects on Acoustic Surface Waves." The technical monitor was Ms. Pamela G. Kinnebrew, Engineer Research and Development Center–Geotechnical and Structures Laboratory (ERDC-GSL).

The work was performed by the Signature Physics Branch and the Engineering Resources Branch of the Research and Engineering Division, US Army ERDC Cold Regions Research and Engineering Laboratory (CRREL). At the time of publication, Mr. Paul M. Kutia and Dr. Melisa Nallar were branch chiefs, respectively; and Dr. Orian Z. Welling was division chief. The acting deputy director of ERDC-CRREL was Ms. M. Kelly Swiderski, and the acting director was Dr. Ivan P. Beckman.

COL Christian Patterson was commander of ERDC, and Dr. David W. Pittman was the director.

1 Introduction

1.1 Background

As part of the US Army Engineer Research and Development Center's (ERDC) Basic Research project "Nonlinear Effects on Acoustic Surface Waves," experimental characterization of porous media is a key research task. Porosity is a fundamental transport property that describes the amount of air contained within a material. This report focuses on the air within the material that is accessible from the exterior, that is, open porosity, because of its importance to acoustics. A direct, nondestructive measurement method is required to accurately measure the open porosity of porous media.

1.2 Objectives

The goal of this task is to create and analyze a system to measure the open porosity of porous media. Specifically, a design with high accuracy at low cost is the main objective. The system will be a key piece of measurement equipment for years to come in the Cold Regions Research and Engineering Laboratory's (CRREL) Acousto-Optic Laboratory, making durability a significant requirement. The system will additionally take porosity measurements of snow, such that the apparatus must be cold hardened.

1.3 Approach

A critical survey of porosity measurement methods was conducted to determine a suitable technique for a cold room environment. Given a suitable measurement method, specific system requirements were then defined. An initial uncertainty analysis was performed to quantify subcomponent specifications. This allowed for the system to be engineered and subsequently built. After system fabrication, a postfabrication uncertainty analysis was performed to determine whether system requirements were met, and the ability to accurately measure porosity.

2 Survey of Methods

Many methods exist for measuring porosity, such as directly (bulk volume measurement followed by a solid volume measurement), or by optical, imbibition, mercury injection, density, and gas expansion approaches (Dullien 1979). Methods based on gas expansion provide direct, nondestructive measurement of open pore air volume with high accuracy, and in a cost-effective manner. All gas expansion methods rely on Boyle's Law for an isothermal process. Four methods based on Boyle's Law were identified and compared.

The first method was proposed by Beranek and involves an isolated test chamber to hold a specimen (Beranek 1942). A manometer (to measure pressure) is connected to the test chamber with the other end connected to the ambient environment. A pressure or volume change is induced by raising one side of the manometer. The amount of air in the specimen is calculated using the readings of the manometer (to get pressure and volume changes) and then applying Boyle's Law.

Beranek's system was improved on by Champoux et al. (1991) by eliminating the pressure reference to ambient conditions, and instead uses a pressure reference to a reference chamber. The Champoux et al. (1991) system eliminates the need for a manometer through use of a differential pressure transducer and a micrometer head-driven piston, for pressure measurement and volume displacement, respectively. Boyle's Law is again used to calculate the amount of air in the sample.

Leclaire et al. (2003) improved on Beranek et al.'s (1942) and Champoux et al.'s (1991) designs by accounting for additional thermal effects. Leclaire et al.'s (2003) design features a reference chamber and sample chamber connected to one another with a manometer. The reference chamber is filled with solid volume to create a comparable air volume to the sample chamber, which should be similarly affected by thermal effects. A volumetric change is applied to both chambers through use of a water-drawing piston connected to the manometer. The water is repeatedly drawn while varying the air volume of the test chamber using a separate volume-adjustment piston. When the volume of air in both chambers is equal, the measurement read by the manometer, after drawing water, will read as no difference, and the amount of solid material in the test

specimen is the amount read by the volume-adjustment piston in the test chamber—from which the air volume in the sample can be calculated.

Salissou and Panneton (2007) also proposed a system based on the ideal gas law for an isothermal process. Their system uses a test chamber connected to a vacuum pump and argon tank, which can create low and high pressure states, respectively. The pressure in the test chamber is measured using a digital manometer connected to ambient pressure. The mass of the chamber is measured using a mass balance. The mass and pressure of the test chamber are measured at four states, a variation of high and low pressure, with and without the porous sample in the test section. From these four measurements, the solid volume of the sample can be calculated, assuming an isothermal process with the ideal gas law.

Based on the survey of gas expansion methods, the design of Champoux et al. (1991) was most suitable for current and future research objectives. The system is simple and does not require repetitive procedures for measuring the porosity of a sample. Specifically, the design reduces the influence of pressure changes in ambient conditions by using a reference chamber, and data interpolation accounts for temperature changes (Champoux et al. 1991). The system does not require a noble gas nor a liquid manometer, allowing it to be used in a cold-room environment. An additional consideration is the widespread adoption of the method, which is highly repeatable (Pompoli et al. 2017).

3 Porosity Measurement

Porosity is the fraction of the void space (air) in a porous material compared to the material's total volume. Acoustic applications are typically concerned with a material's effective porosity, or the porosity that is open to the exterior of the material. Porosity is defined as

$$\Omega = \frac{V_a}{V_t}, \tag{1}$$

where Ω is the porosity of the sample, V_a is the volume of air in the sample, and V_t is the total volume of the sample.

The total volume of the sample is defined as

$$V_t = V_a + V_m, \tag{2}$$

where V_m is the volume of solid material in the sample.

The Champoux et al. (1991) design, shown in Figure 1, uses a reference chamber connected to a test chamber. The two chambers are connected via tubing to a differential pressure transducer, which measures the pressure difference between the two. The design features a test section with a porous specimen held within. The test section includes the air within the specimen as well as a residual volume of air that is contained within the excess space in the test chamber, tubing, fittings, seals, and the measurement section of the differential pressure transducer.

Figure 1. Schematic diagram of porosimeter.

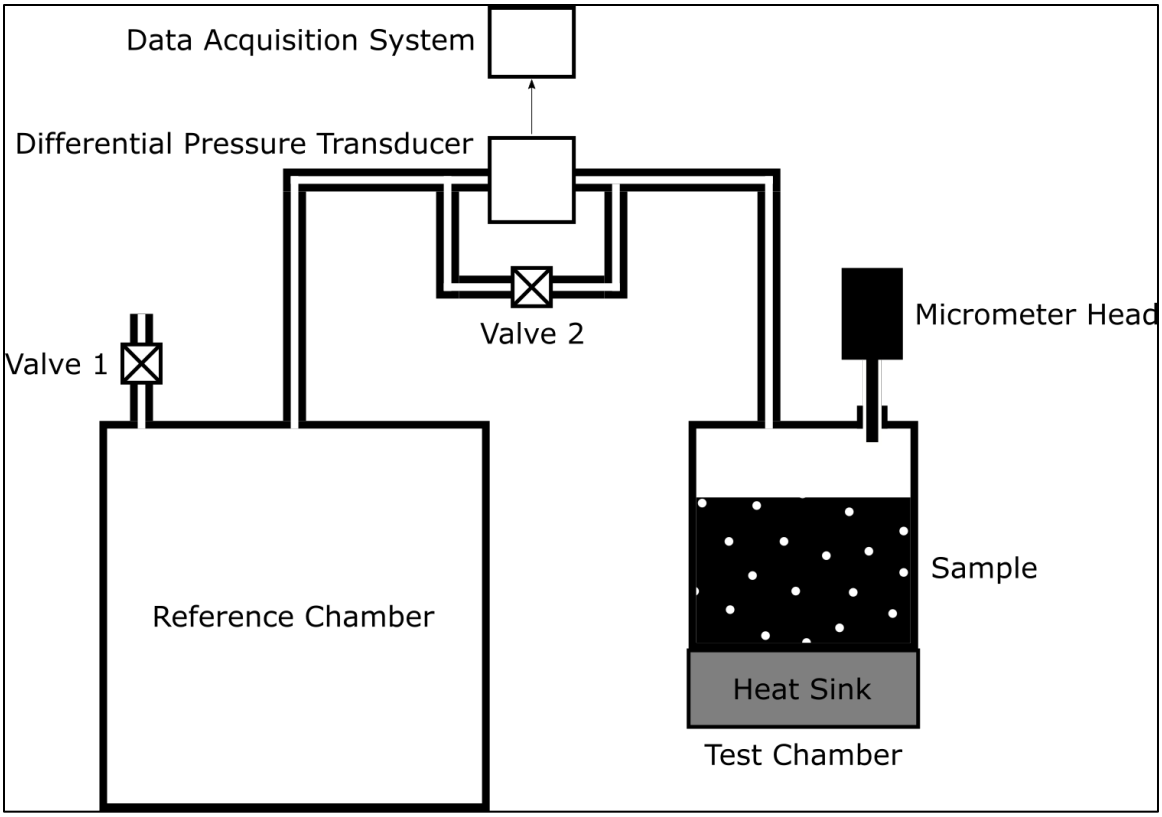

When the volume, and subsequently the pressure, of the test section changes, compliance of the gaskets, seals, and the diaphragm of the differential pressure transducer leads to volume changes which cannot be measured directly. In the test section, a relation of volumes is

$$V_a = V - V_e, \tag{3}$$

where V is the apparent total volume of air in the test chamber and V_e is the effective residual volume.

The effective residual volume is defined similar to the actual residual volume and related to the apparent measured volume of air in the test section. This volume is found through a calibration process detailed in Section 3.1 of this report.

The volume of air within the test chamber is changed through movement of a piston, driven by a micrometer head. This allows for precise adjustment of air volume in the test section. The volume change caused by the piston is,

$$\Delta V = \frac{\pi d^2}{4} \Delta x, \tag{4}$$

where d is the diameter of the piston and Δx is the linear displacement of the piston.

By changing the air volume within the test section, it is assumed that an isothermal process for gas expansion and compression holds, which is the basis for Boyle's Law. From the ideal gas law, temperature being held constant, the apparent total volume of air from a known volume change and a measured pressure change is,

$$V = -\frac{P_0 + \Delta P}{\Delta P} \Delta V, \tag{5}$$

where P_0 is the initial pressure, ΔP is the change in pressure between the test section and the reference chamber, and ΔV is the change in volume. Knowing the effective residual volume, total sample volume, and the total apparent air volume from Equation (5), the overall porosity of the sample can be calculated from Equations (3) and (1).

The measurement process involves first opening both valves to ambient pressure. The valve exposing the reference chamber to ambient air is then closed to isolate the system from any possible variations in the ambient pressure. The valve separating the two sections of the apparatus is then closed, isolating the two from each other. Volume compression is then induced by turning the micrometer head for a given displacement that corresponds to the desired volume change. Displacement of the piston (attached to the micrometer head) is performed slowly to mitigate thermal effects due to the pressure change and piston movement. As the volume change occurs, the differential pressure is measured and recorded continuously to account for any small thermal effects which cannot be avoided. Once the volume change concludes, and ample time passes to allow for the settling of any dynamic response in the differential pressure (such as an initial overshoot), the recording can be concluded.

The thermal effects present as an asymptotic linear change in differential pressure, which can be accounted for by linear regressions on data before and after a volume change. Interpolation can be performed across the linear regressions to determine the overall change in pressure. After interpolating, the porosity can be calculated using the change in pressure.

3.1 Calibration

The residual volume is defined as the air in the test section of the apparatus that is not contained within the sample (Champoux et al. 1991). An additional effective volume arises from the movement of gaskets and the diaphragm of the differential pressure transducer, when taking a measurement. To account for this, the effective residual volume can be found by leaving the test chamber empty and taking normal measurements as previously described over a range of volume changes. The empty test chamber can be thought of as a case where a material sample has a porosity of one. Knowing this, the effective residual volume can be calculated using Equations (3) and (1).

3.2 Theoretical Uncertainty Analysis

An uncertainty analysis was conducted to determine design requirements. This analysis, similar to that by Champoux et al. (1991), estimates how accurately porosity can be measured and its range of measurement.

For a quantity with combined uncorrelated inputs, uncertainty is defined as (ISO/IEC 2008)

$$u_c^2(y) = \sum_{i=0}^{n} \left(\frac{\partial f}{\partial x_i}\right) u^2(x_i), \tag{6}$$

where u_c is the combined standard uncertainty of the quantity, y is the estimate of the measurand, f is the function defining the quantity, x_i is the input, and u is the uncertainty of the input.

For independent, identically distributed sources of error the total variance is equal to the sum of each error's variance (Papoulis 1991, 184–188). Taking the standard deviation of a measurement as its uncertainty yields the following expression

$$u_c^2(y) = \sum_{i=0}^{n} u_n^2, \tag{7}$$

where u_n is the uncertainty from a specific source.

Using Equations (1) and (6), the uncertainty in the measurement of porosity is,

$$\left(\frac{\delta\Omega}{\Omega}\right)^2 = \left(\frac{\delta V_a}{V_a}\right)^2 + \left(\frac{\delta V_t}{V_t}\right)^2, \quad (8)$$

where $\delta\Omega$, δV_a and δV_t are the uncertainties of porosity, the volume of air in the sample, and the total volume of the sample, respectively.

Uncertainty of the air volume, within the porous sample, is

$$\delta V_a^2 = \delta V^2 + \delta V_e^2, \quad (9)$$

where δV and δV_e are the uncertainties of the total air volume and residual volume, respectively. The uncertainty in the volume of the sample is dependent on the accuracy to which it is measured. This relationship is

$$\left(\frac{\delta V_t}{V_t}\right)^2 = \left(\frac{\delta t}{t}\right)^2 + \left(\frac{2\delta d_s}{d_s}\right)^2, \quad (10)$$

where t is the thickness of the sample, d_s is the diameter of the sample, δt is the uncertainty in the thickness of the sample, and δd_s is the uncertainty in the diameter of the sample.

The uncertainty in the volume of the air in the test section is

$$\left(\frac{\delta V}{V}\right)^2 = \left(\frac{\delta P_0}{P_0+\Delta P}\right)^2 + \left(\frac{P_0\Delta P}{\Delta P(P_0+\Delta P)}\right)^2 + \left(\frac{\delta\Delta V}{V}\right)^2, \quad (11)$$

where δP_0 is the uncertainty in the initial pressure, and $\delta\Delta P$ is the uncertainty in the change in pressure. The uncertainty of the initial pressure δP_0 is based on the accuracy of the ambient pressure transducer and the digitization system used to measure its output. All uncertainties are independent, identically distributed sources of error. The uncertainty of the initial pressure is

$$\delta P_0 = \sqrt{\delta P_a^2 + S_{P_a}^2 \delta U_d^2}, \quad (12)$$

where δP_a is the uncertainty of the analog output of the ambient pressure transducer, S_{P_a} is the sensitivity of the ambient pressure transducer (pressure per voltage), and δU_d is the uncertainty from the digitization system used for measurement.

The uncertainty in the differential pressure is similar to that of the ambient pressure, however, an additional uncertainty arises from interpolating the change across the linear regressions of the differential pressure time series, which defines the experimental change in pressure ΔP. The uncertainty of the differential pressure measurement, $\delta\Delta P$, is

$$\delta\Delta P = \sqrt{S_{\Delta P}^2(\delta U_t^2 + \delta U_d^2) + \delta U_i^2}, \tag{13}$$

where $S_{\Delta P}$ is the sensitivity of the differential pressure transducer (pressure per voltage), δU_t is the uncertainty from calibration of the transducer, and δU_i is the uncertainty from the linear regressions.

The uncertainty of the change in volume of air in the test section is

$$\left(\frac{\delta\Delta V}{\Delta V}\right)^2 = \left(\frac{\delta\Delta x}{\Delta x}\right)^2 + \left(\frac{2\delta d}{d}\right)^2. \tag{14}$$

With the exception of Equations (10), (13), and (14) (as they were not part of the analysis done by Champoux et al. 1991), this uncertainty analysis can reproduce Figure 5 from Champoux et al. (1991, 914). Recreating Figure 5 serves as confirmation of the uncertainty analysis. Assuming the maximum possible volume change of 0.309 cm^3, relative uncertainty in measured porosity as a function of sample volume is shown in Figure 2.*

* For a full list of the spelled-out forms of the units of measure used in this document, please refer to *US Government Publishing Office Style Manual*, 31st ed. (Washington, DC: US Government Publishing Office, 2016), 248–52, https://www.govinfo.gov/content/pkg/GPO-STYLEMANUAL-2016/pdf/GPO-STYLEMANUAL-2016.pdf.

Figure 2. A reproduction of the theoretical uncertainty as depicted in Fig. 5 of Champoux et al. (1991). Relative uncertainty for porosity $\delta\Omega/\Omega$ is based on experimental uncertainties reported in Champoux et al. (1991), and a volume change of 0.309 cm³. The *dashed line* represents a differential pressure of 0.3 mmHg, as shown in the original figure. (Image reproduced from Champoux et al. 1991. CC BY 4.0.)

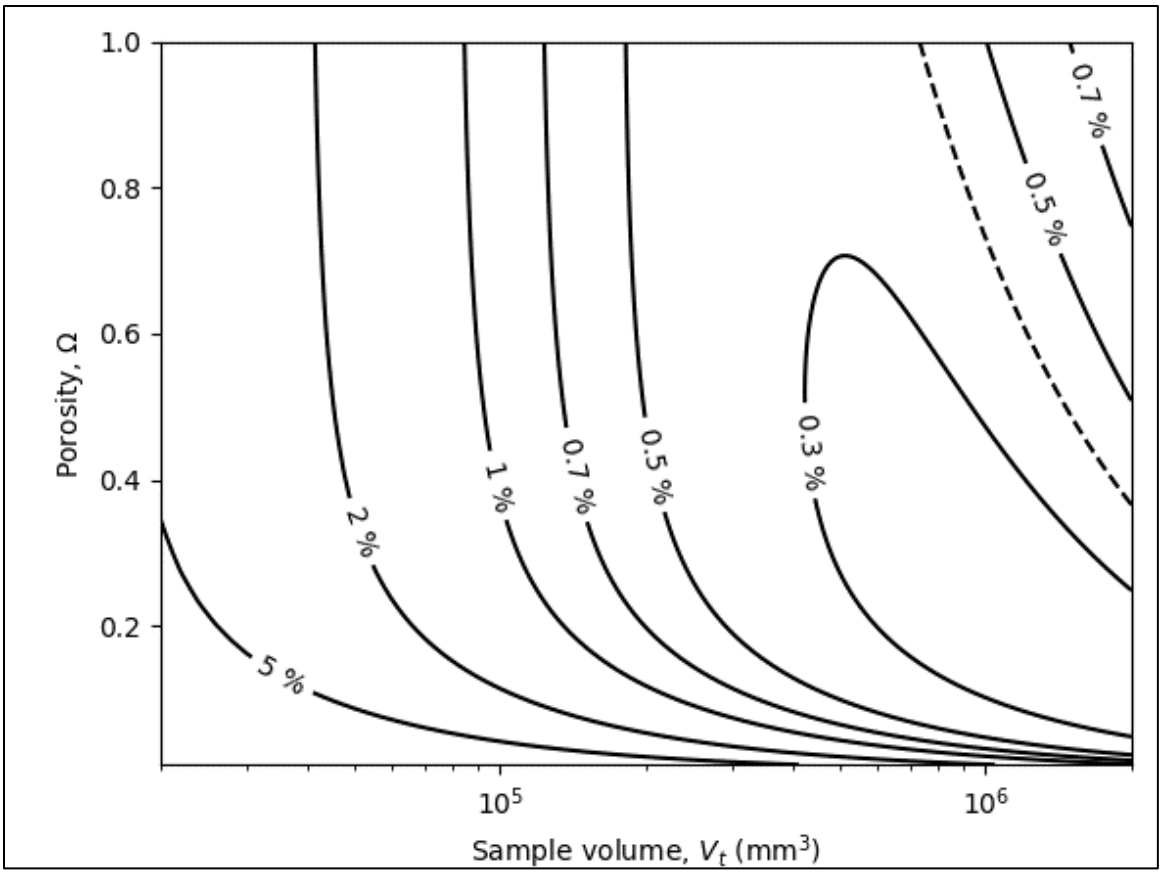

4 Porosimeter Design

The porosimeter design closely follows that of Champoux et al. (1991), with changes made to meet specific design requirements. A full design model is shown in Figure 3.

Figure 3. Three-dimensional model of porosimeter. *RC* represents the reference chamber, *PT* represents the differential pressure transducer, *MH* represents the micrometer head, and *HS* represents the heat sink. The test chamber is directly above the heat sink and cannot be seen from this diagram.

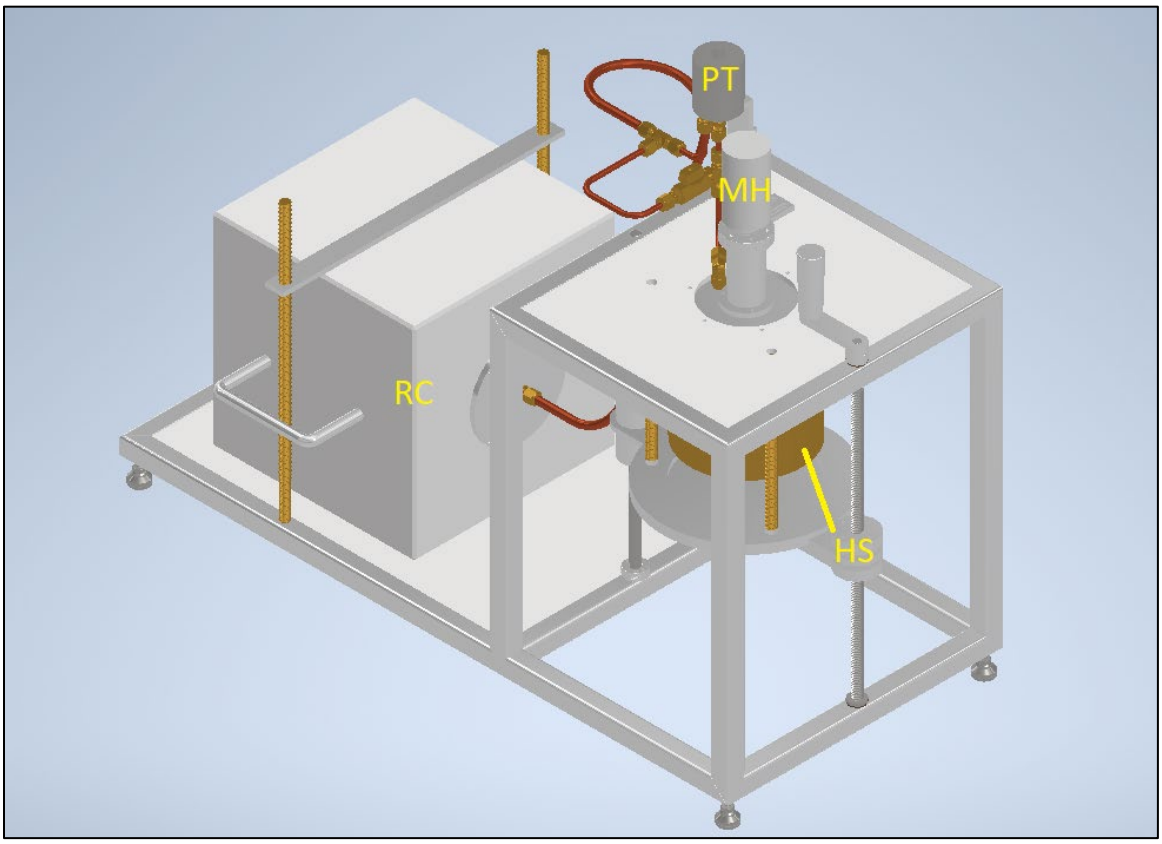

4.1 Temperature Considerations

To support measurements of snow, the porosimeter must be able to take measurements at temperatures as low as −10°C. This primarily impacts selection of a differential pressure transducer.

4.2 Frame

A frame was designed to hold components of the porosimeter, and allow for transport as a single unit. The frame consists of aluminum square tubing welded together. A large plate provides a base for the reference

chamber. The reference chamber is fixed in place using two brass threaded rods and a mounting bracket. The test chamber is raised allowing for the sensitive instrumentation (differential pressure transducer and micrometer head) to be held in place while accessing the test chamber. A plate, fixed to the top side of the test section portion of the frame, provides mounting points for the top plate of the test chamber and the bracket for the differential pressure transducer. The frame surrounding the test chamber holds hardware in place for the raising and lifting mechanism of the test section.

4.3 Lifting Mechanism

A lifting mechanism allows for easy movement of the test section's heavy heatsink. The system uses a lifting plate, which is guided on one side by a linear shaft and linear bearings, which is raised or lowered on the opposite side by an acme threaded rod and compatible nuts. The linear bearings are held in place through tube shaped brackets and internal retention rings. Acme nuts are held in place by plates that compress them against the lifting plate. This allows the nuts to be rotated, prior to compression against the lifting plate, which prevents binding caused by misalignment between the two nuts along the threaded rod. The linear shaft is connected to the frame of the apparatus using two-piece shaft collars, with one collar fixed to the frame. The threaded rod is connected to the frame with bronze bushings. A handle is attached to the top of the acme threaded rod for rotation. The Acme threaded rod is machined in a way that it can be slightly lifted, with respect to the frame and bushings, to allow for final tightening of the test chamber without interference from the threaded rod.

4.4 Test Chamber

A test chamber was designed to hold a wide variety of porous media and allow for easy removal. The design involves an aluminum tube which is held on either side with mounting plates. Internal dimensions of the chamber were a diameter of 100 mm and depth of 55 mm to allow for measurement of a 50 mm thick sample. An internal diameter of 100 mm was selected because it is common to other measuring equipment, for example, transmission impedance tube, and airflow resistivity meter. The tube design also permits removal of stuck samples. The chamber can measure solid samples and granular samples. A top plate was designed to seal the test chamber, and provide ports for the piston and differential pressure transducer. The top plate is fixed to the frame of the apparatus

and is used to mount the micrometer head bracket. A cylindrical extrusion provides a mechanical stop for a reproducible fit (and internal test chamber volume) each time the chamber is opened and closed.

The bottom of the test chamber has a similar extrusion as to the top, and is connected to a large piece of brass. The large brass piece acts as a heat sink to the test chamber to promote isothermal conditions for the gas compression process. The heat sink sits on top of the raising and lifting mechanism and is prevented from moving in the horizontal plane by a groove in the lifting plate. After a coarse height adjustment with the lifting mechanism, the test chamber is sealed tight using three brass rods and wingnuts clamping the chamber together with its top plate.

4.5 Micrometer Head

A micrometer head permits fine adjustments of the volume displacement piston. Through uncertainty analysis and market research, a translational accuracy of 2 μm was a reasonable requirement for the micrometer head. Exceeding 2 μm accuracy leads to a small reduction of uncertainty, but incurs a much higher cost. Translational accuracy was considered in conjunction with specifications for the volume displacement piston, as they both affect uncertainty in the volume change by Equation (14). The micrometer head selected is a Mitutoyo, 152–348, which has a linear displacement accuracy of 2 μm with a total displacement range of 25 mm. The flat-tipped head couples to the displacement piston with a shaft coupler, and the mounting stem clamps to a bracket that holds it in place. The head is oversized with large, laser-etched scales.

The micrometer head is held in place using a bracket with a shaft collar that clamps to the mounting stem of the micrometer head. The tip of the micrometer is connected to the piston using a shaft coupler designed for aligned shafts. The bracket was designed to keep the micrometer head stable in all three axial directions, as even a slight movement in any direction can lead to a change in air volume within the test chamber.

4.6 Piston

To create a change in the air volume of the test section a piston system was implemented. A cylindrical piston with diameter of 0.75 in. results in a low value of uncertainty when measuring porosity. Through market research, a diameter tolerance of 0.001 in. proved to be a reasonable requirement.

The piston was machined in a two-tier design (change in diameter half-way through) to provide the correct diameter for volume displacement on one side and to provide a surface which can be clamped to the micrometer head on the other side.

4.7 Tubing

Copper tubing was used to provide air connections between the different parts of the apparatus. The tubing is strong but also malleable enough to be bent to desired positions. Copper tubing is also suitable for low environmental temperatures.

4.8 Fittings

Yor-Lok tube fittings (from McMaster-Carr) and NPT (National Pipe Taper) fittings were used for tubing connections. The Yor-Lok fittings provide a strong and airtight connection to the tubing without a need for sealant and allow tubing to be rotated within for precise positioning. The Yor-Lok fittings also permit the differential pressure transducer to be removed for maintenance or calibration. NPT fittings are used in locations where fittings are connected to one another or directly to a part of the apparatus.

4.9 Seals

The seals were chosen to ensure an airtight fit for all moving and removable parts of the system. A Teflon based sealant was chosen for all threaded connections which were required to be airtight. O-rings were chosen as a simple and cost effective system for creating seals for the piston, test chamber, and plates on the reference chamber. O-rings were specifically chosen for these points as they may require movement and removal during regular use. A polyurethane O-ring, along with grease for dynamic applications, was chosen to seal the piston. Viton O-rings, appropriate for static applications, were chosen for all other seals. The Parker O-Ring Handbook was used to dimension all O-ring glands and mating surfaces, according to recommendations for static and dynamic situations (Parker Hannifin Corporation 2021).

4.10 Differential Pressure Transducer

A differential pressure transducer was chosen to provide high enough accuracy and span to confidently measure porosity. A Setra, Model ASL

was chosen due to its high accuracy over a wide range of temperatures. The transducer has an accuracy of 0.07% full-scale (FS) and a compensated temperature range down to −20°C. The 0 to 2 in. water column (WC) range was chosen as it is able to measure a wide range of porosities with a low value of uncertainty.

The differential pressure transducer is held in place using a two-piece bracket with adjustment grooves to account for misalignment of the transducer and tubing. The transducer is mounted vertically with ports facing downward per the manufacturer's calibration procedure.

4.11 Digitization System

A digitization system was chosen to provide a high enough accuracy and range to confidently measure the output of the differential pressure transducer. The digitizer chosen was a Campbell Scientific, CR1000 Datalogger. This was chosen due to its high accuracy and wide temperature use range. The CR1000 has an accuracy of 0.12% of reading +2 mV with a temperature range down to −25°C. The system has an analog input range of ±5 V at 13-bits, with a maximum sampling frequency of about 83 Hz. Measurement uncertainty does not limit the accuracy of the differential pressure transducer.

4.12 Reference Chamber

The reference chamber was designed to provide a reference pressure for the test chamber, derived from its initial state. It was designed to have a similar volume to that of the Champoux et al. (1991) design, with a total volume of about 14,000 cm^3. The reference chamber has removable plates to attach different fittings for use with other test equipment. It can be removed and transported with handles.

4.13 Ambient Condition Measurements

Ambient temperature and pressure were measured using a Vaisala PTU300 environmental monitor. The environmental monitor has accuracies of 0.35°C and 60 Pa (for analog outputs). The monitor outputs analog measurements of temperature and pressure in real-time, which are measured by the digitization system simultaneously with the analog output of the differential pressure transducer.

5 Design Uncertainty

Uncertainty plots were used to determine design parameters and if certain pieces of equipment were acceptable for the system. These plots quantify the expected uncertainty for a wide range of sample volumes and all possible sample porosity values. Accuracy of the total system can be evaluated according to component specifications. After design requirements were determined, a final uncertainty plot was created as shown in Figure 4. The dashed line in Figure 4 represents the maximum range of the differential pressure transducer such that measurements to the left of the line would exceed the transducer's range. Figure 4 estimates measurements of porosities greater than 0.2, for samples larger than 200,000 mm^3, can be obtained with an accuracy of 0.5% to 1%.

A preliminary requirement of the system was to hold a sample of 393.4 cm^3 (100 mm diameter cylinder at 50 mm thick) to allow for samples to fit into additional measurement equipment. A detailed plot of this uncertainty is shown in Figure 5. Measurements of porosities greater than 0.2 can be obtained with an accuracy of 0.4% to 0.6%.

Uncertainty values used for plot generation are shown in Table 1. The value of effective residual volume, its uncertainty, and the uncertainty in data interpolation were chosen to be the same as Champoux et al. (1991). Actual values could only be determined after construction and calibration of the porosimeter.

Table 1. Uncertainty values used for preliminary design uncertainty analysis.

Parameter	Uncertainty
Effective Residual Volume, V_e	28,700 mm^3
Sample Thickness, t	0.03 mm
Sample Diameter, d_s	0.03 mm
Ambient Pressure Analog Output, P_a[1]	60 Pa
Digitization System, U_d	0.12% of reading + 0.002 V
Differential Pressure Calibration, Ut	0.07% FS (0.0035 V for 5-V sensor)
Interpolation Process, U_i	0.133 Pa (0.001 mmHg)
Piston Displacement, Δx	0.002 mm
Piston Diameter, d	0.0004 in. (0.01 mm)

[1] The ambient pressure analog output has an output range of 0–5 V over 95,000–105,000 Pa.

Figure 4. Contour plot of relative uncertainty (*solid lines*) in porosity for a porosimeter with different total sample volumes (assuming a sample completely fills the sample holder) and different porosities. The volume change, induced by the micrometer-driven piston, is assumed to be 0.5 cm³. The *dashed line* represents the maximum pressure limit of the differential pressure transducer. The area to the *left* of the dashed line cannot be measured, as it would exceed the maximum differential pressure range.

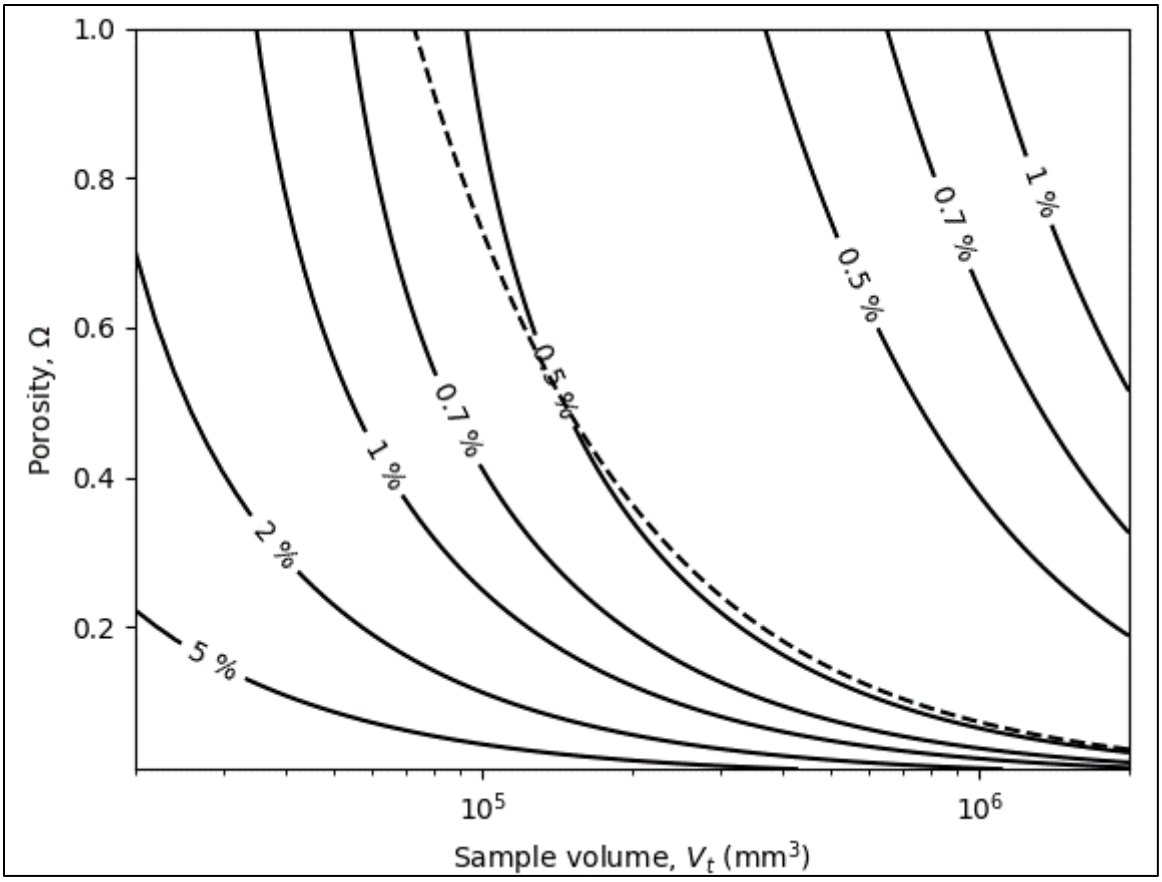

Figure 5. Relative uncertainty in porosity measurement for a sample of 393.4 cm^3, with a micrometer-driven piston-induced volume change of 0.5 cm^3. Samples with a porosity smaller than indicated by the *dashed vertical line* cannot be measured, as it would exceed the range of the differential pressure transducer.

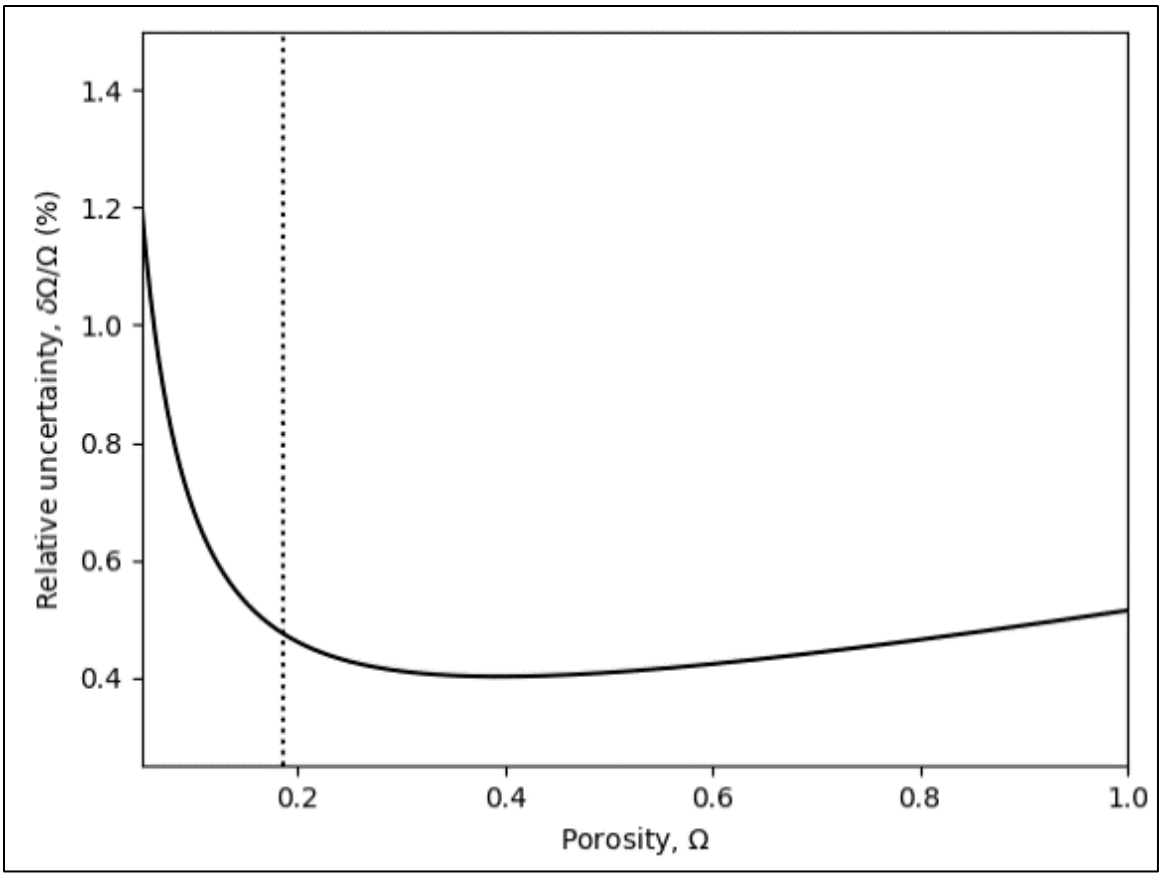

6 Experimental Design

6.1 Test Plan

To test the effectiveness of the porosimeter, a wide variety of materials were measured and compared to known porosities. Each measurement followed the procedure described in Section 3 of this report.

The type of material and variations on each type are given in Table 2. The solid aluminum cylinders are a form of measurement standards since the measured porosity can be directly compared to the geometry of each sample. Ball bearings, glass beads, and sintered plastic were chosen to compare measured porosity to that estimated by the mass and density of the solid material. The filter foam was chosen to compare measured porosity to water displacement measurements. Three samples of each variation were measured, except for the solid aluminum cylinders.

Table 2. Materials measured with variations in material types.

Material	Variations
Solid Aluminum Cylinder	86.6 mm diameter by 50 mm height (0.75 sample volume), 70.8 mm diameter by 50 mm height (0.50 sample volume), 50 mm diameter by 50 mm height (0.25 sample volume)
Steel Ball Bearings	1/8 in. diameter, 5/32 in. diameter, 3/16 in. diameter
Glass Beads	approximately 4 mm diameter
HDPE Sintered Plastic	200 µm pores, 300 µm pores, 400 µm pores, 500 µm pores
Polyether Filter Foam	10 pores per inch (ppi), 20 ppi, 30 ppi

The first step in the measurement process was to perform a calibration to determine the effective residual volume, as detailed in Section 3.1. After, preliminary measurements were taken to test what displacements were within the range of the differential pressure transducer. Once the range was determined, approximately 300 measurements were taken to estimate the average value of the residual volume as well as its standard deviation. The residual volume's standard deviation was then used in a final calculation of uncertainty for the system.

After calibration, water displacement measurements were taken on the glass beads and filter foam. Filter foams with 40 pores per inch (ppi), or higher, were unable to fully saturate with water. A 5 mL micropipette,

adjustable down to 0.01 mL with 0.01 mL accuracy, was used to fill a 100 mm diameter 50 mm depth glass dish to full capacity and its volume was recorded. The samples solid volume could then be measured by placing a sample in the dish and repeating the process.

Measurements with the porosimeter were taken for each of the porous samples at varying piston displacements. The variation in piston displacement was conducted to observe whether estimated porosity depends on differential pressure.

6.2 Analysis Plan

Once measurements were taken, post processing was performed to estimate porosity of a sample from measurements. All analysis was performed using the programming language Python. The interpolation procedure first required manual picking of the following events (time-windowing) in the differential pressure time series: closing of the valves; the start of a linear trend in differential pressure; the start of piston displacement; and the start of another linear trend in differential pressure once piston displacement ceases. The time at which the valves close is when the initial pressure inside the porosimeter is equivalent to ambient pressure. The time-series between the start of a linear trend in differential pressure, and the start of piston displacement, defines a region for linear regression before piston displacement. The point where the differential pressure change becomes linear, after piston displacement ceases, is the starting point for another region of linear regression. This second region, for linear regression, continues to the end of the measurement. A linear least-squares method was used for regression. The differential pressure change was calculated by extending both lines and finding the difference between the two, halfway between when piston displacement began and when the differential pressure trend became linear after piston displacement ceases. With the measured pressure change, ambient conditions, and geometric sample measurements, the porosity can be calculated.

7 Results

7.1 Calibration and Adjusted Residual Volume

A calibration procedure was performed to measure the effective residual volume of the porosimeter. To obtain an estimate of the effective residual volume and its standard deviation, with high confidence, about 300 measurements were taken. In initial testing it was found that there is a large amount of variation in measurements if the differential pressure is less than 250 Pa. Consequently, calibration measurements were only performed for differential pressures above 250 Pa. This limits operation of the system when making measurements over the same range. To achieve differential pressures exceeding 250 Pa, it was found that piston displacements of 4 mm to 7 mm are required. Increments of 0.25 mm displacement were used to simplify the measurement procedure. Results of the calibration showed that the average effective residual volume is 48,200 mm^3 with a standard deviation of 623 mm^3. Raw data and statistical estimates are shown in Figure 6.

After calibration, preliminary measurements (not shown) taken on the aluminum cylinders showed a consistent positive bias in measurements. To attempt to account for this error, an adjustment was made to the effective residual volume to correct for the positive bias. Because the measurements of expected porosity for the solid aluminum samples are based on geometric measurements of the samples, there is high certainty in the known porosity of the test chamber sample volume. The difference in the measured porosities from the geometric porosities can be used to estimate the change in effective residual volume on average. Analysis showed the new effective residual volume to be 49,800 mm^3 (a 1,300 mm^3 increase). This adjusted residual volume was used in all measurements seen in the results section.

Figure 6. Calibration results for the effective residual volume in the porosimeter. Average residual volume was found to be 48,200 mm³ with a standard deviation of 623 mm³. *Black dots* represent individual measurements. The *solid line* represents the average of the measurements and the *dashed line* represents ±1 standard deviation away from the average.

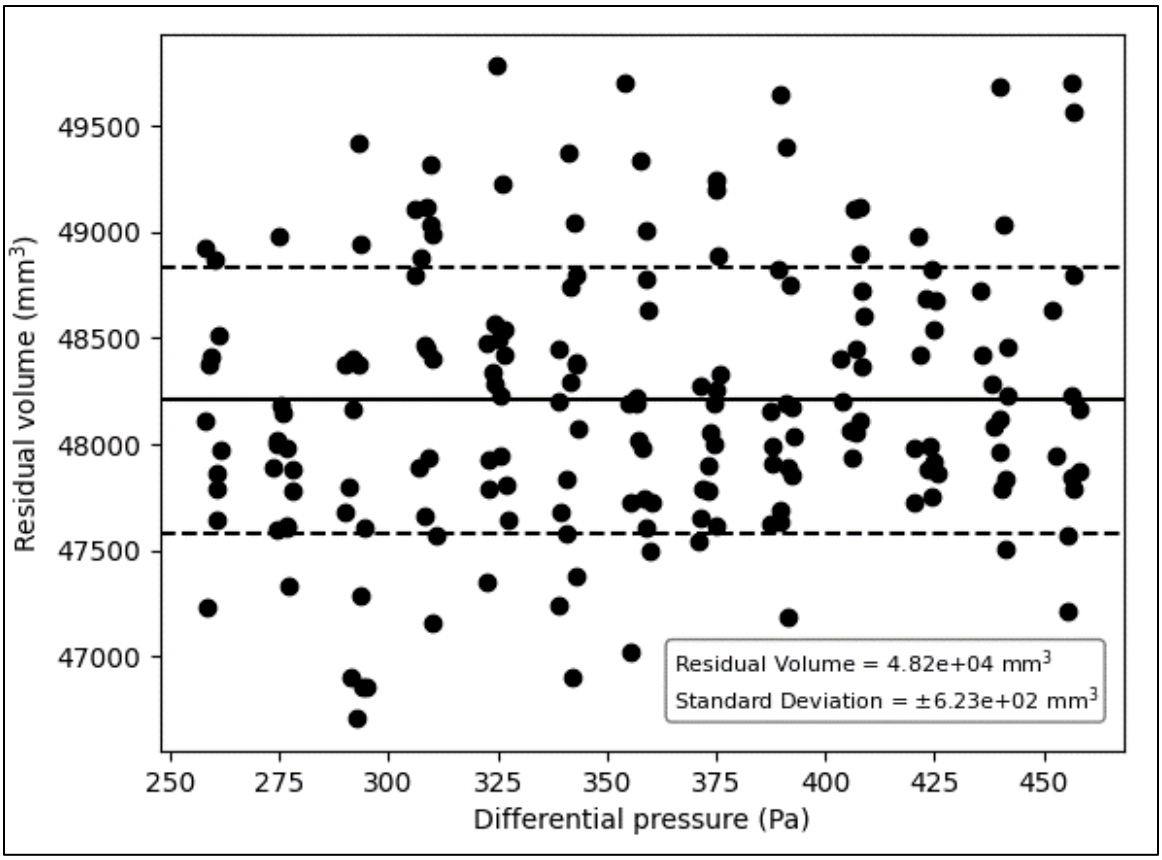

7.2 Interpolation Uncertainty

After taking measurements, the uncertainty component arising from least-squares regression performed in the interpolation process was estimated. A plot showing typical best fit lines for a measurement time-series is shown in Figure 7. The uncertainty from the interpolation was estimated by the standard deviation of the residuals (error), which arise from the line of best fit, as well as combining the uncertainty from before and after the piston displacement as two independent sources of uncertainty. The average standard deviation observed from the interpolation process was 0.837 Pa, which was estimated from calibration measurements.

Figure 7. Example of a linear regression, over two regions of the time series, to measure the change in differential pressure. Differential pressure change is measured at the time in the middle of the step change.

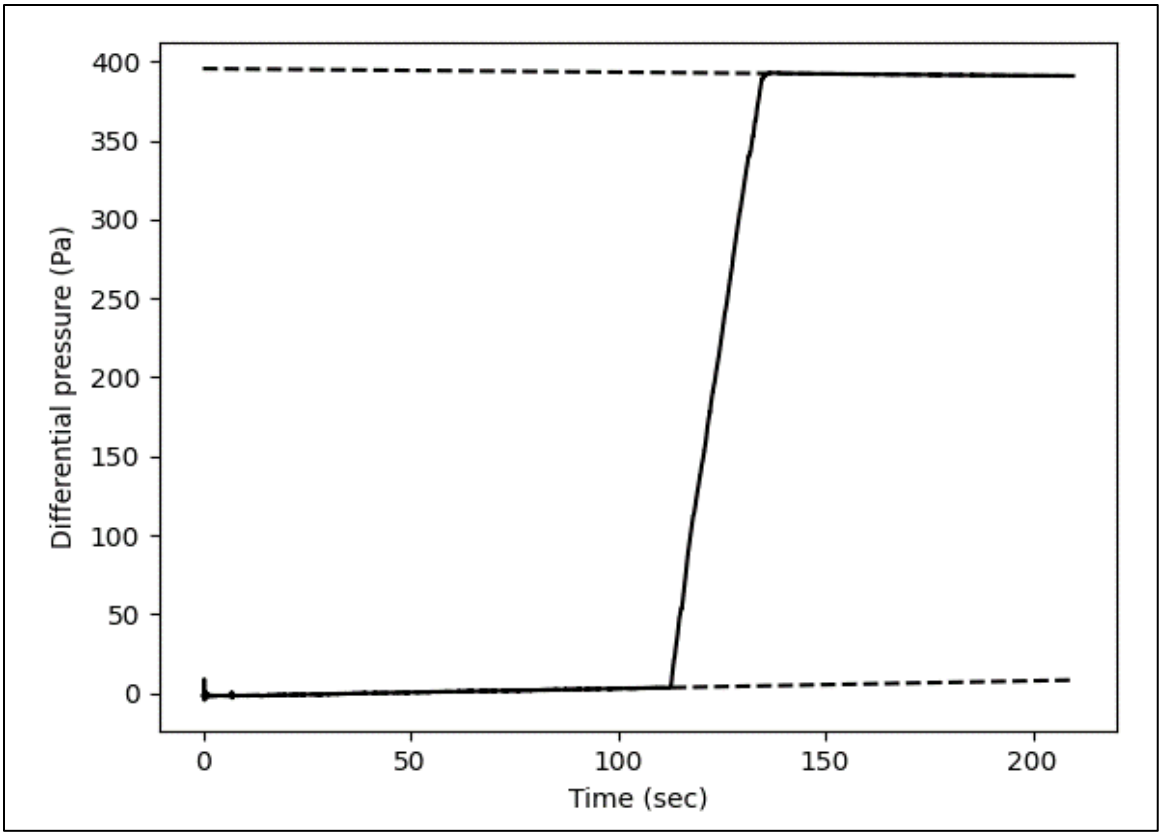

7.3 Updated Uncertainty

After fabricating and assembling the porosimeter system, the uncertainty analysis was repeated with updated values for the effective residual volume and interpolation uncertainties. A chart of the updated values is given in Table 3.

Table 3. Uncertainty values for porosimeter after calibration.

Parameter	Uncertainty
Effective Residual Volume, V_e	49,800 mm^3
Sample Thickness, t	0.03 mm
Sample Diameter, d_s	0.03 mm
Ambient Pressure Analog Output, P_a	60 Pa
Digitization System, U_d	0.12% of reading + 0.002 V
Differential Pressure Calibration, Ut	0.07% FS (0.0035 V for 5-V sensor)
Interpolation Process, U_i	0.837 Pa (0.006 mmHg)
Piston Displacement, Δx	0.002 mm
Piston Diameter, d	0.0004 in. (0.01 mm)

Using the uncertainty values from Table 3, the uncertainty plots are updated as seen in Figures 8 and 9. It can be seen that the overall uncertainty is larger than the prebuild analysis. However, for the specific sample volume of interest the system is able to measure samples, having a porosity greater than 0.2, with an accuracy of about 0.8% to 1.0% over that range.

Figure 8. Updated contour plot of relative uncertainty in porosity for a porosimeter with different total sample volumes (assuming a sample completely fills the sample holder) and different porosities. The volume change, induced by the micrometer-driven piston, is assumed to be 0.5 cm^3. The *dashed line* represents the maximum pressure limit of the differential pressure transducer. The area to the *left* of the dashed line cannot be measured, as it would exceed the maximum differential pressure.

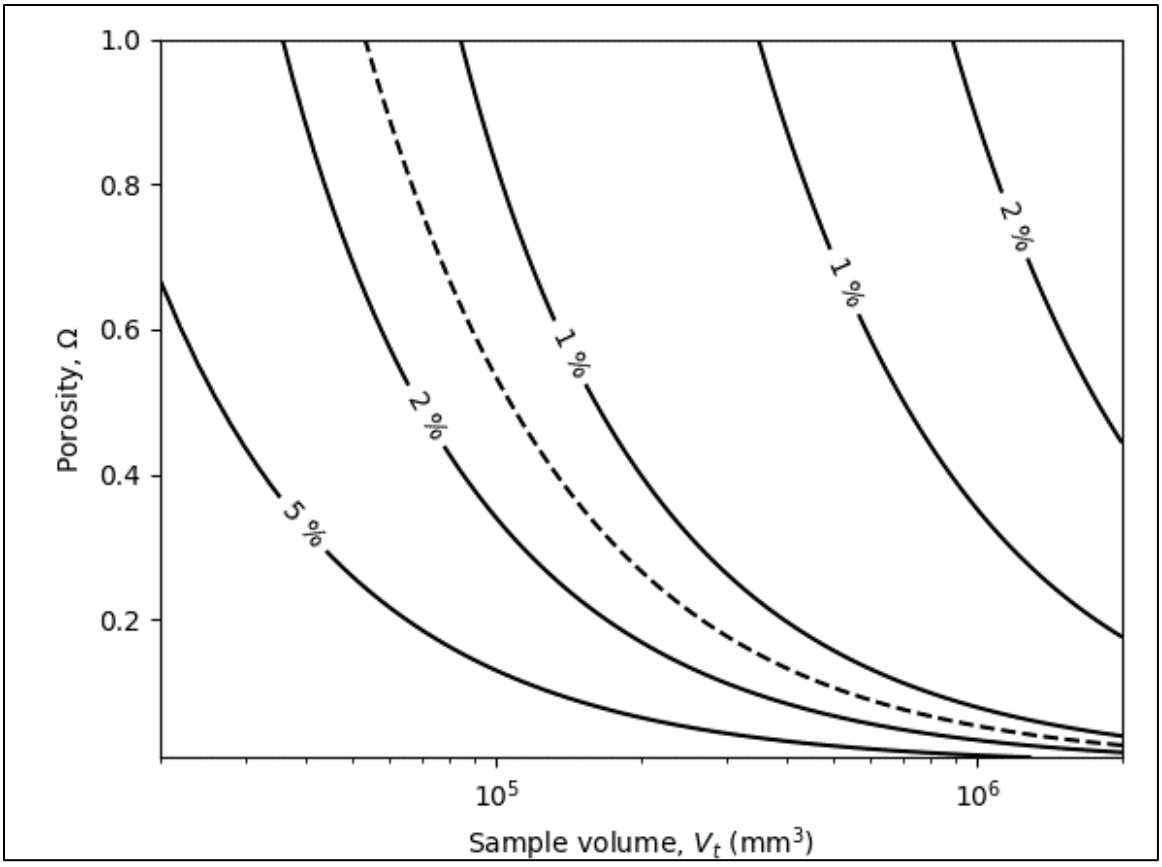

Figure 9. Updated relative uncertainty in the porosity measurement for a sample of 393.4 cm³, with a volume change, induced by the micrometer-driven piston, of 0.5 cm³. Samples with a porosity smaller than indicated by the *dashed line* cannot be measured, as it would exceed the range of the differential pressure transducer.

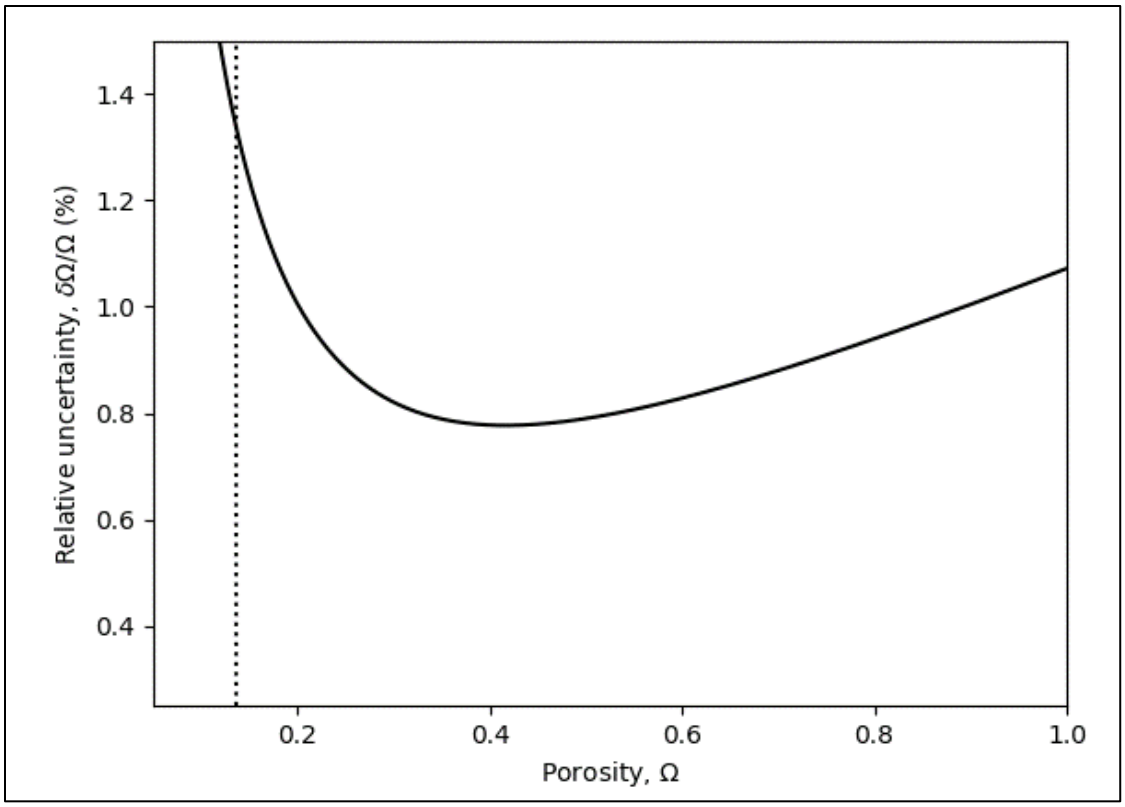

7.4 Displacement Ranges

Through uncertainty analysis not shown, it was found that measuring at a maximum differential pressure leads to the lowest amount of uncertainty in measurement. This can be seen in Equations (8) to (11) where an increase in ΔP leads to a decrease in the final value of uncertainty for porosity. Therefore, for a given porosity there is an ideal piston displacement that leads to a maximum differential pressure, within the measurement range. Since it is not realistic to have a large number of different displacements when measuring porosity, a few piston displacements were chosen to measure over specific porosity ranges. This simplifies the measurement process because the exact porosity is usually unknown prior to measurements. Selected porosity ranges and near-ideal piston displacements are given in Table 4. Uncertainties for a given porosity can then be estimated as seen in Figure 10. The uncertainty decreases as the porosity increases with ranges of 0.75% to 0.50% in the 0.25 to 0.50 porosity range, 0.45% to 0.40% in the 0.50 to 0.75 porosity range, and 0.36% to 0.34% in the 0.75 to 1.00 porosity range.

Table 4. Piston displacements for different values of sample porosity. Generally, higher porosities require larger piston displacements.

Porosity	Piston Displacement
0.25–0.50	2.5 mm
0.50–0.75	4 mm
0.75-1.00	5.75 mm

Figure 10. Relative uncertainty in porosity for the three different sample porosity ranges in Table 4.

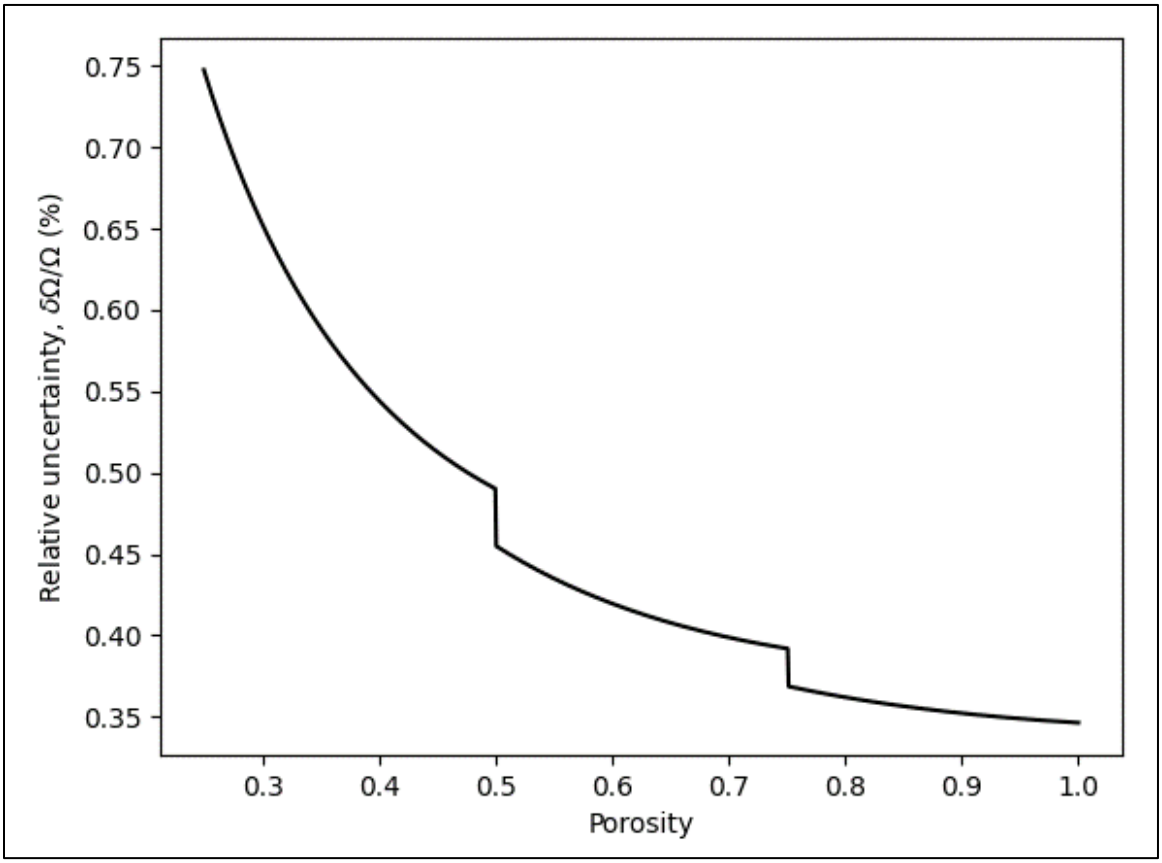

7.5 Solid Aluminum

The first samples measured were solid aluminum cylinders. The cylinders were machined with a smooth surface to allow for accurate estimations of solid volume by caliper measurements. The aluminum samples also serve to check the performance of the porosimeter during future measurements, that is, to monitor any potential drift in accuracy over time. Measurement results are shown in Figures 11 to 13. In all porosity measurement figures, the solid line represents the expected porosity and the dashed lines represent the range of uncertainty in the porosimeter measurement.

In general, the porosity measurements on the solid aluminum samples showed good agreement with the expected values from geometric measurements with an overall lack of bias. This is expected as initial porosity measurements were used to adjust the effective residual volume of the apparatus as part of the calibration procedure. All measurements were contained within the range of the expected uncertainty.

Figure 11. Porosimeter measurements of a solid aluminum cylinder with dimensions of 86.57 mm in diameter and 50.05 mm in height. The *solid line* indicates expected porosity based on measurements of the sample geometry, and the *dashed lines* indicate the expected range of uncertainty.

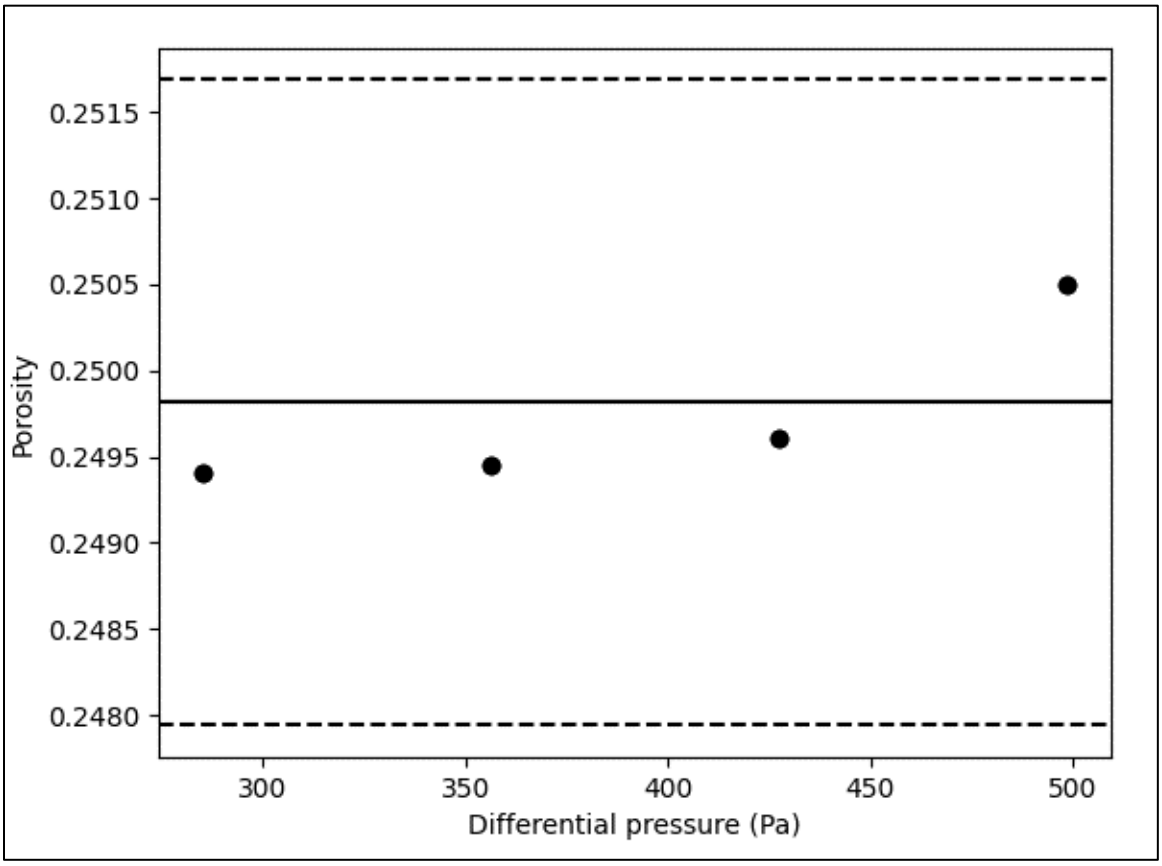

Figure 12. Porosimeter measurements of a solid aluminum cylinder with dimensions of 70.77 mm in diameter and 49.93 mm in height. The *solid line* indicates the expected porosity based on measurements of the sample geometry, and the *dashed lines* indicate the expected range of uncertainty.

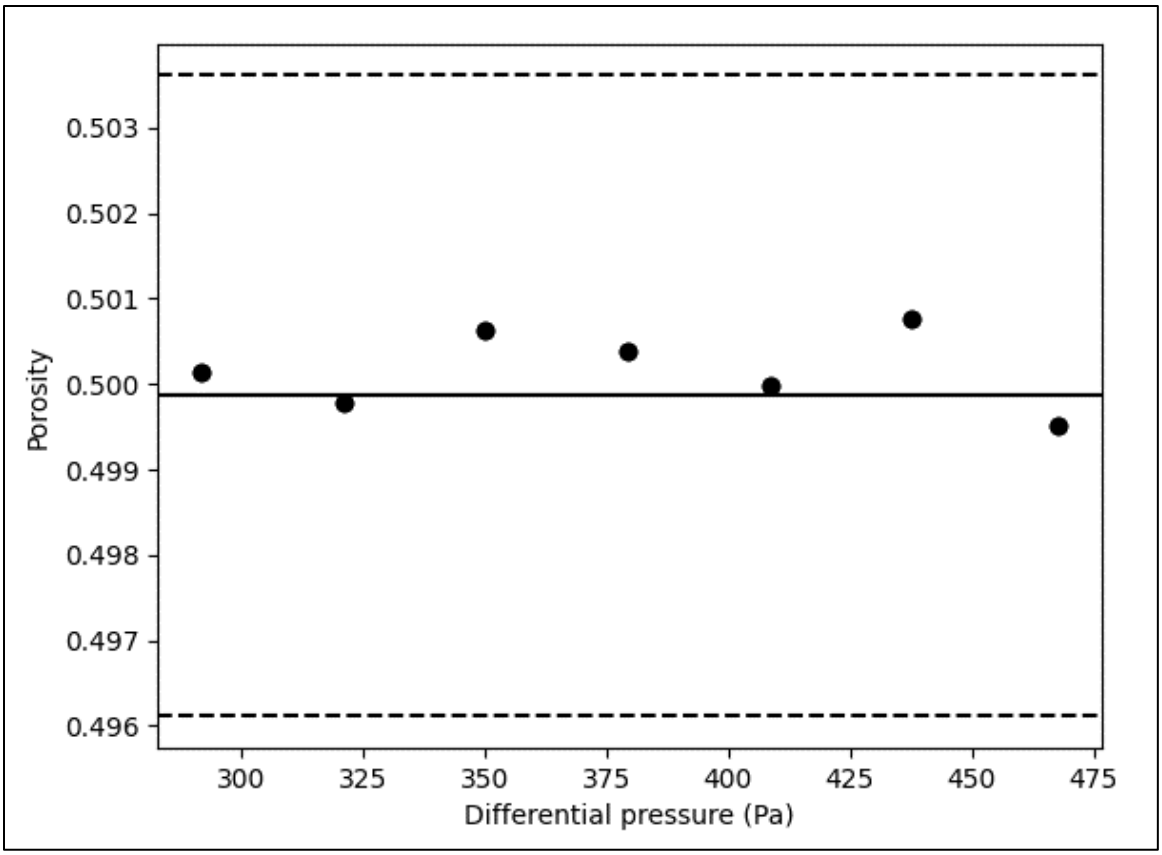

Figure 13. Porosimeter measurements of a solid aluminum cylinder with dimensions of 49.99 mm in diameter and 49.98 mm in height. The *solid line* indicates the expected porosity based on measurements of the sample geometry, and the *dashed lines* indicate the expected range of uncertainty.

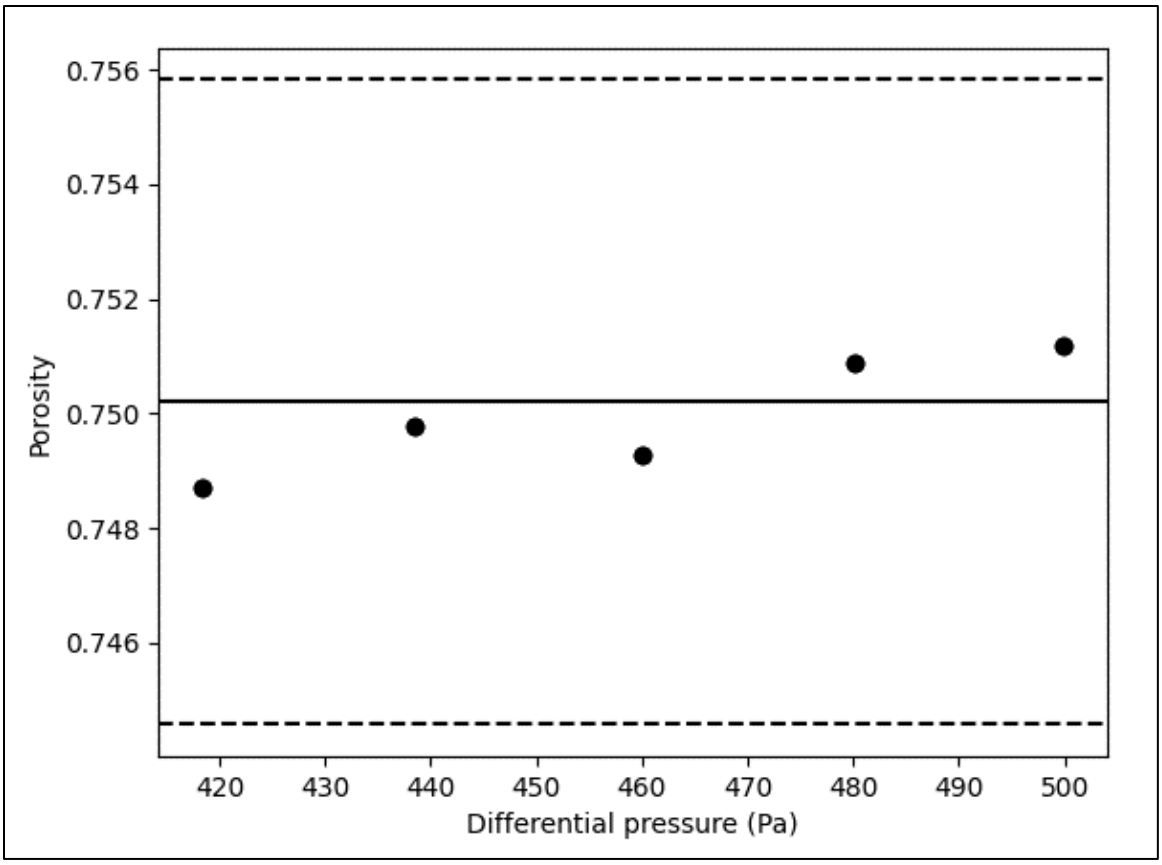

7.6 Ball Bearings

Ball bearings of various diameters were used as granular porous samples. Bearing diameters of 1/8 in., 5/32 in., and 3/16 in. were used. All bearings were made of low carbon steel with a high polish surface. The amount of solid volume was estimated using the mass of each sample and the density of low carbon steel. Measurement results are shown in Figures 14 to 16.

Similar to the aluminum cylinders, porosity measurements on the ball bearing samples showed good agreement with the expected porosity. Most measurements were contained within the range of the expected uncertainty, with more inaccuracy as the diameter of the bearings decreased. For repeated samples of the same diameter ball bearings the measured porosity changed similarly with the expected porosity.

Figure 14. Three sample porosimeter measurements of low-carbon steel ball bearings with diameters of 1/8 in. The *solid lines* indicate expected porosity based on mass measurement, and the *dashed lines* indicate the expected range of uncertainty.

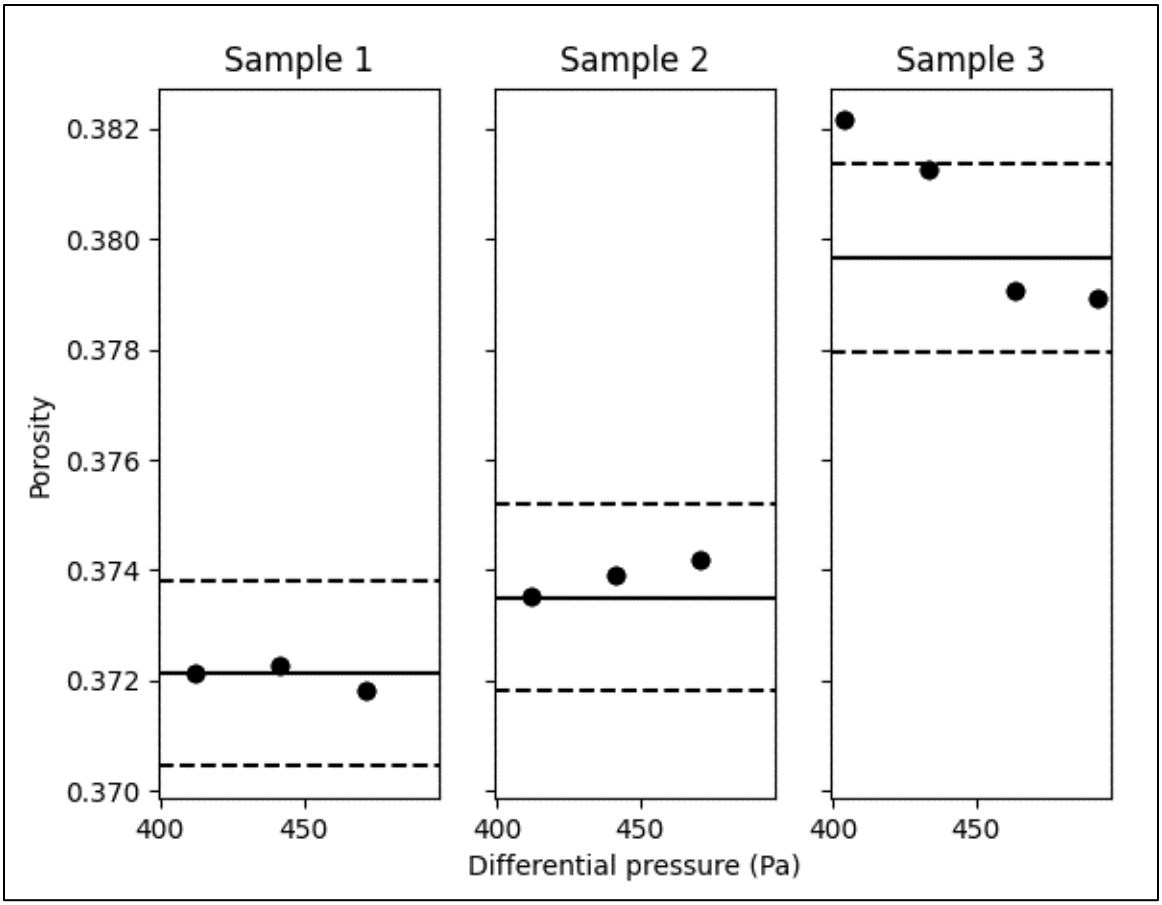

Figure 15. Porosimeter measurements of low-carbon steel ball bearings with diameters of 5/32 in. The *solid lines* indicate expected porosity based on mass measurement, and the *dashed lines* indicate the expected range of uncertainty.

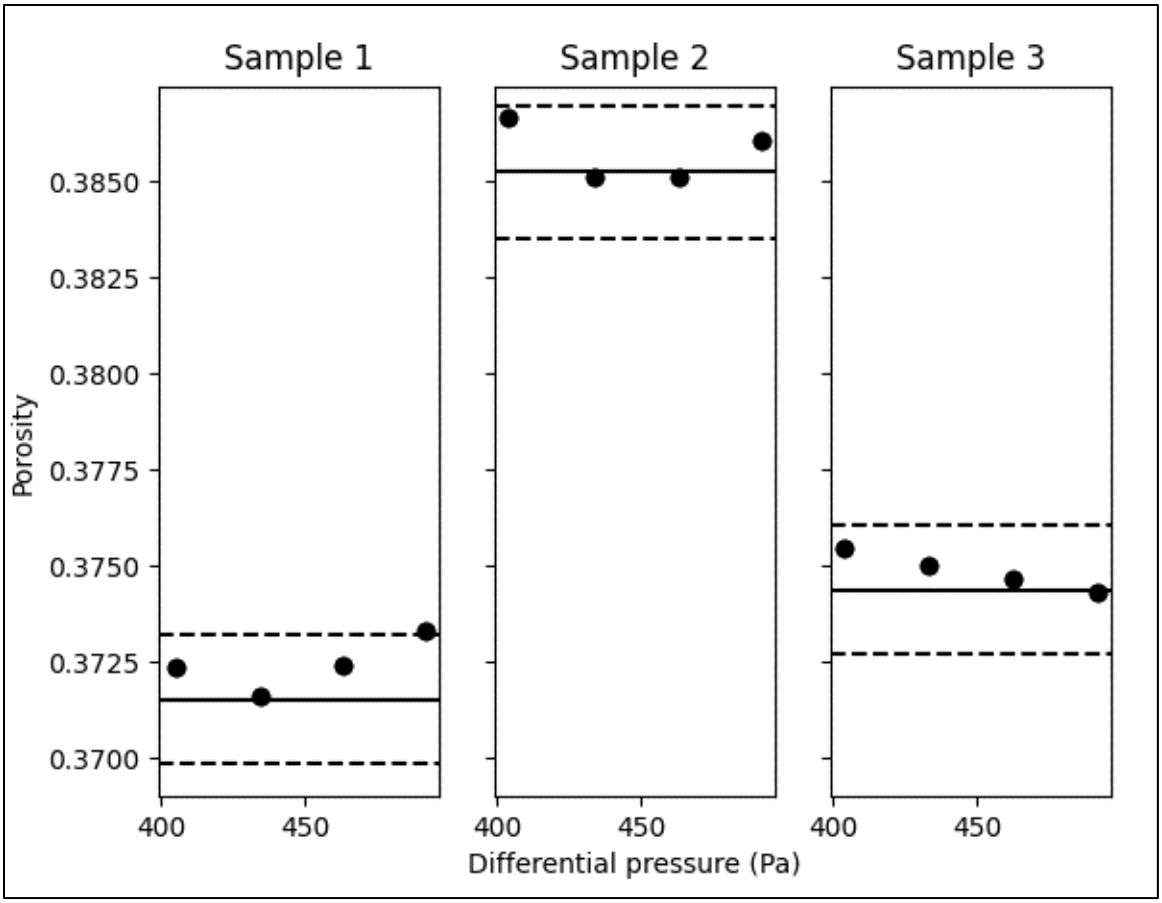

Figure 16. Porosimeter measurements of low-carbon steel ball bearings with diameters of 3/16 in. The *solid lines* indicate expected porosity based on mass measurement, and the *dashed lines* indicate the expected range of uncertainty.

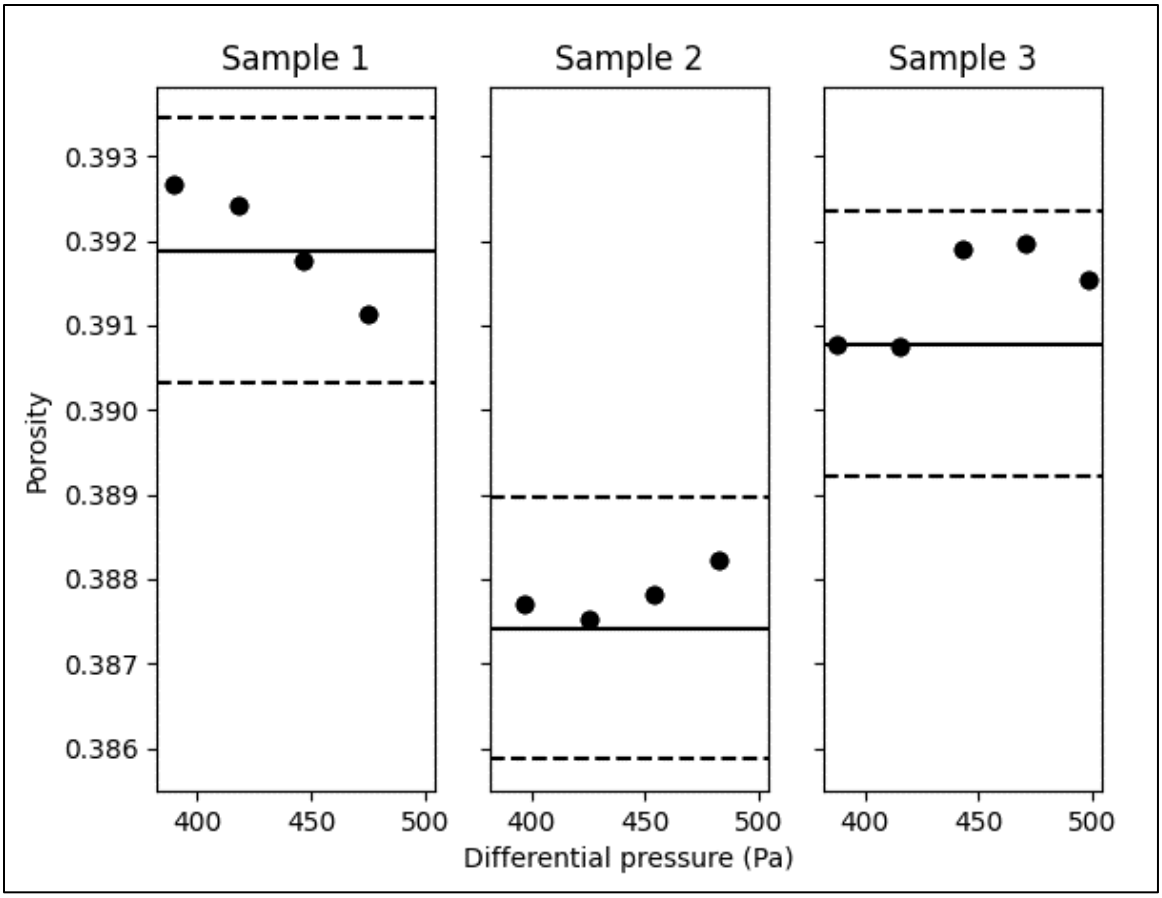

7.7 Glass Beads

Glass beads, of approximately 4 mm diameter, were used as granular porous samples. The amount of solid volume was estimated using the mass of each sample and the density of glass. Measurement results are shown in Figure 17.

The measured porosity of the glass beads shows a positive bias when compared to the expected porosity. Changes in expected porosity resulted in similar changes to measured porosity.

Figure 17. Porosimeter measurements of glass beads with diameters of approximately 4 mm. The *solid lines* indicate expected porosity based on mass measurement, and the *dashed lines* indicate the expected range of uncertainty.

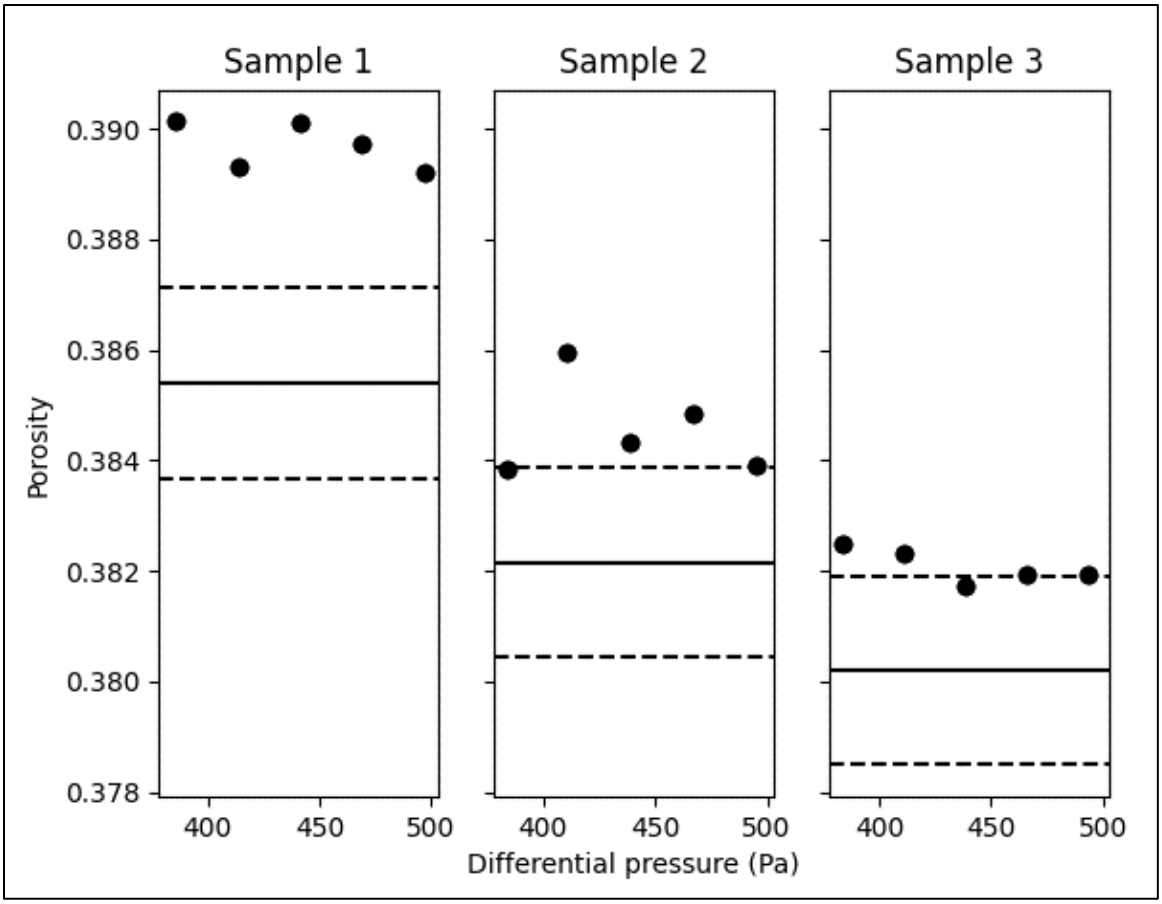

7.8 Sintered Plastic

High-density polyethylene sintered plastic was used as a porous sample. Pore sizes ranged from 200 to 500 μm, in 100 μm increments. The amount of solid volume was estimated using the mass of each sample and the density of polyethylene. Measurement results are shown in Figures 18 to 21.

The measured porosity of the high-density polyethylene slightly exceeded the upper bounds of the expected porosity uncertainty, with changes in expected porosity resulting in similar changes in measurement. The sintered plastic measurements became less accurate as the porosity decreased. All measurements of sintered plastic resulted in the largest inaccuracies to the expected porosity for all sample types.

Figure 18. Porosimeter measurements of sintered plastic with a 200 µm pore size. The *solid lines* indicate expected porosity based on mass measurement, and the *dashed lines* indicate the expected range of uncertainty.

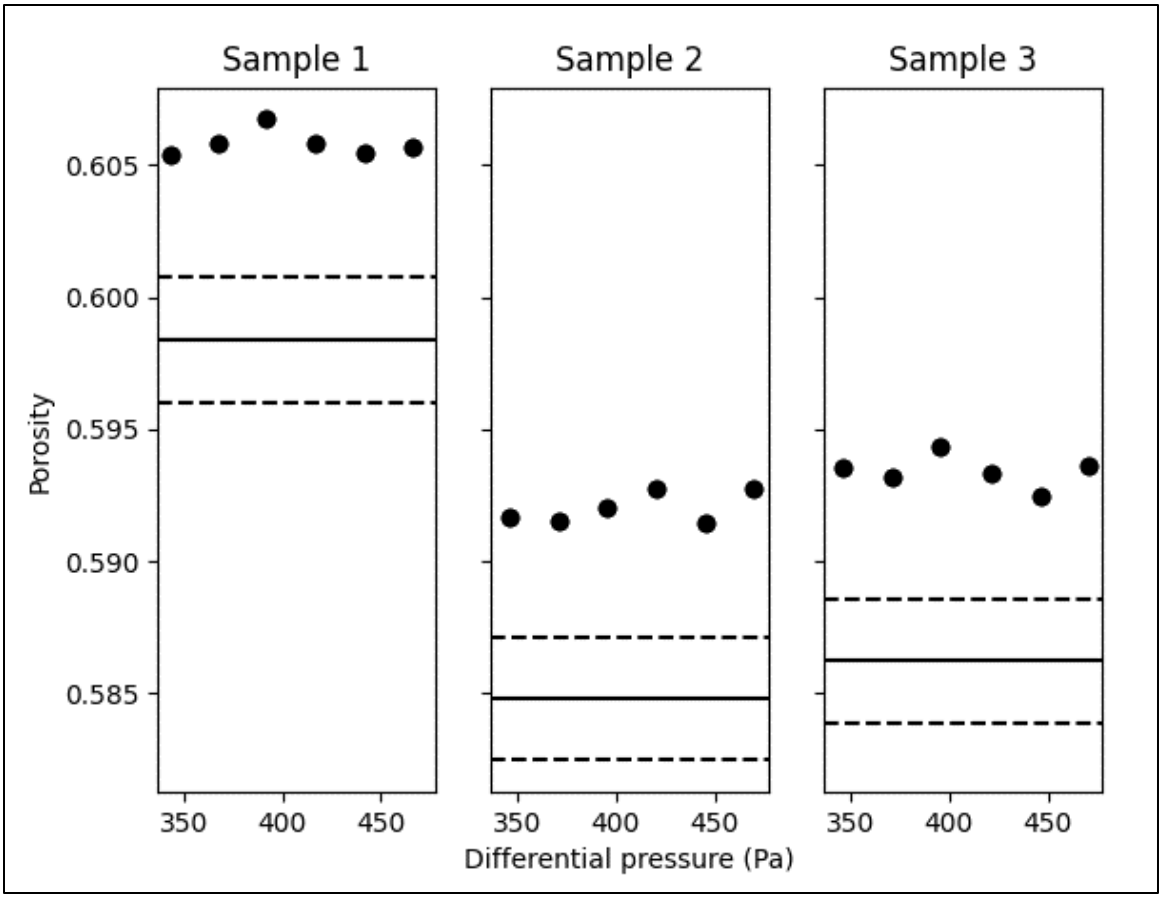

Figure 19. Porosimeter measurements of sintered plastic with a 300 µm pore size. The *solid lines* indicate expected porosity based on mass measurement, and the *dashed lines* indicate the expected range of uncertainty.

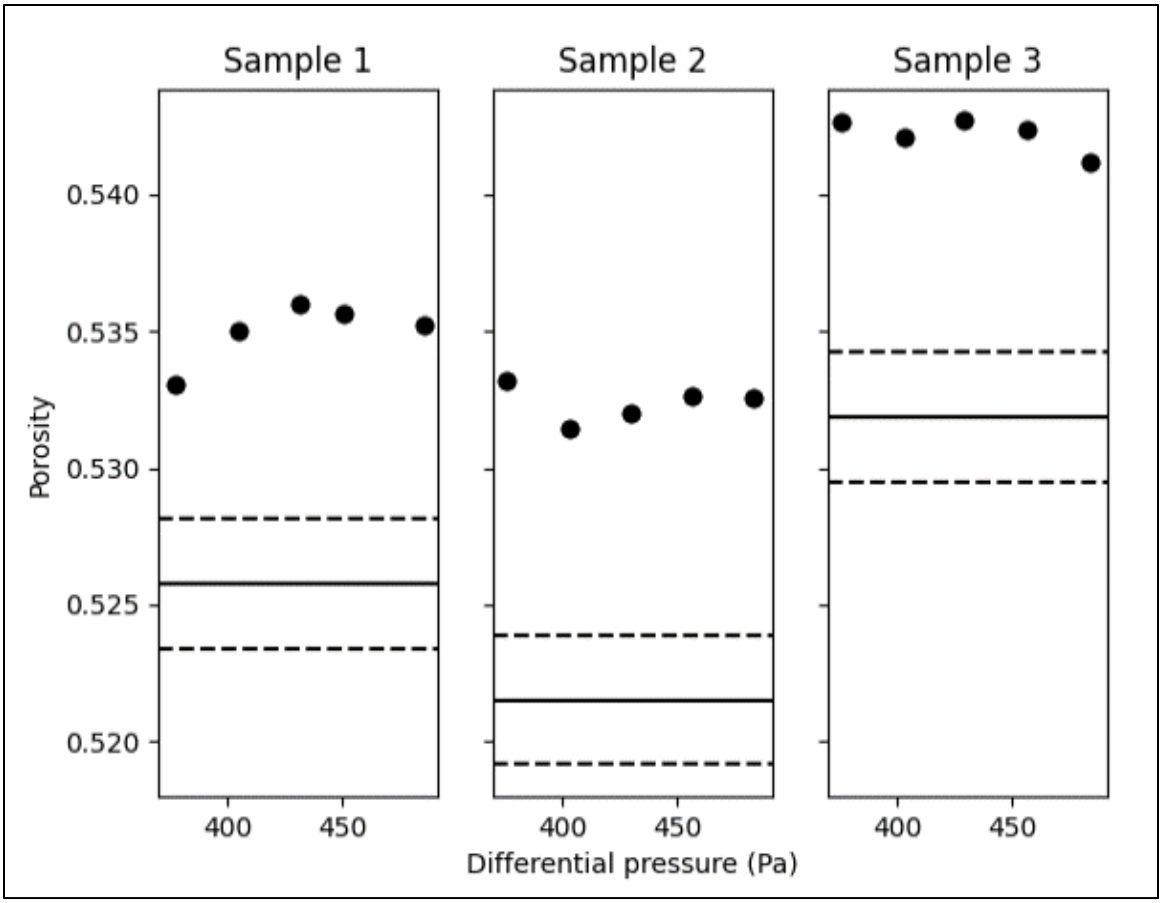

Figure 20. Porosimeter measurements of sintered plastic with a 400 µm pore size. The *solid lines* indicate expected porosity based on mass measurement, and the *dashed lines* indicate the expected range of uncertainty.

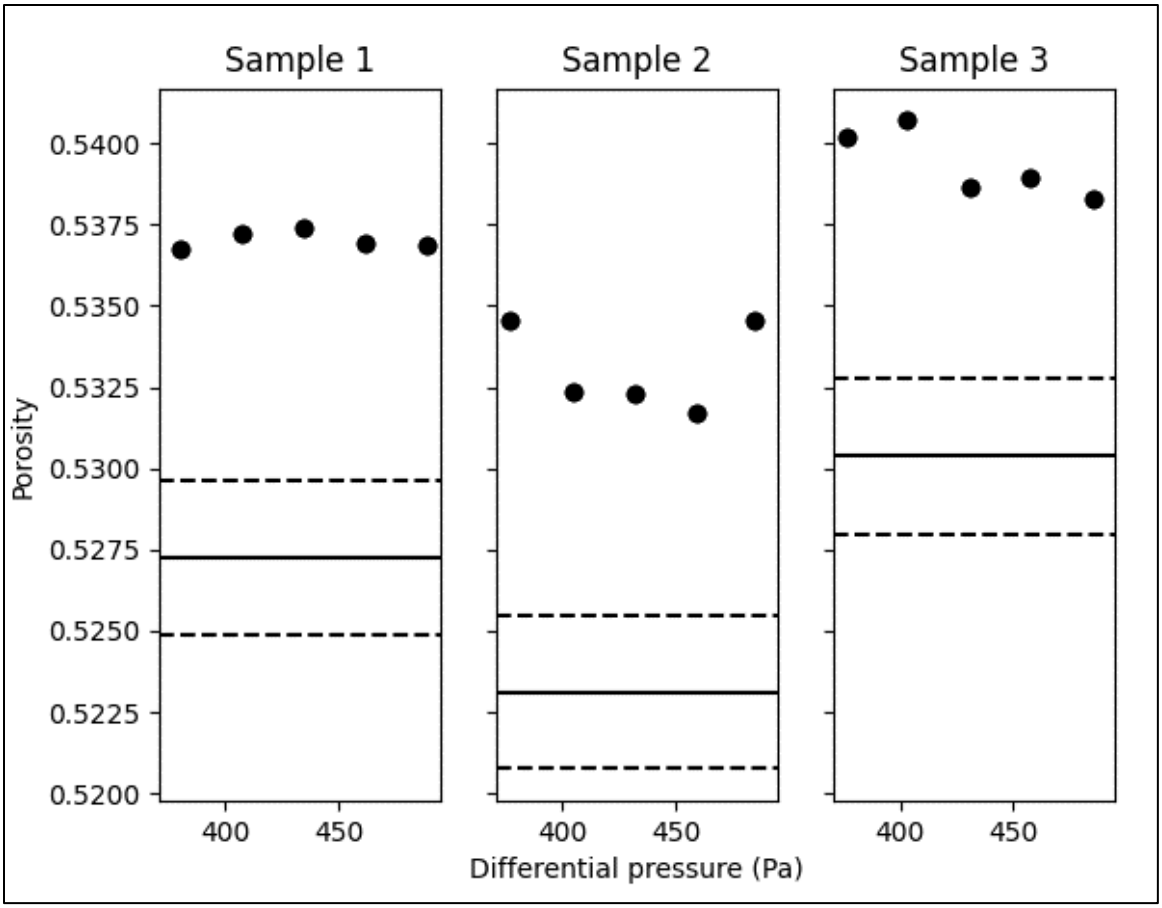

Figure 21. Porosimeter measurements of sintered plastic with a 500 µm pore size. The *solid lines* indicate expected porosity based on mass measurement, and the *dashed lines* indicate the expected range of uncertainty.

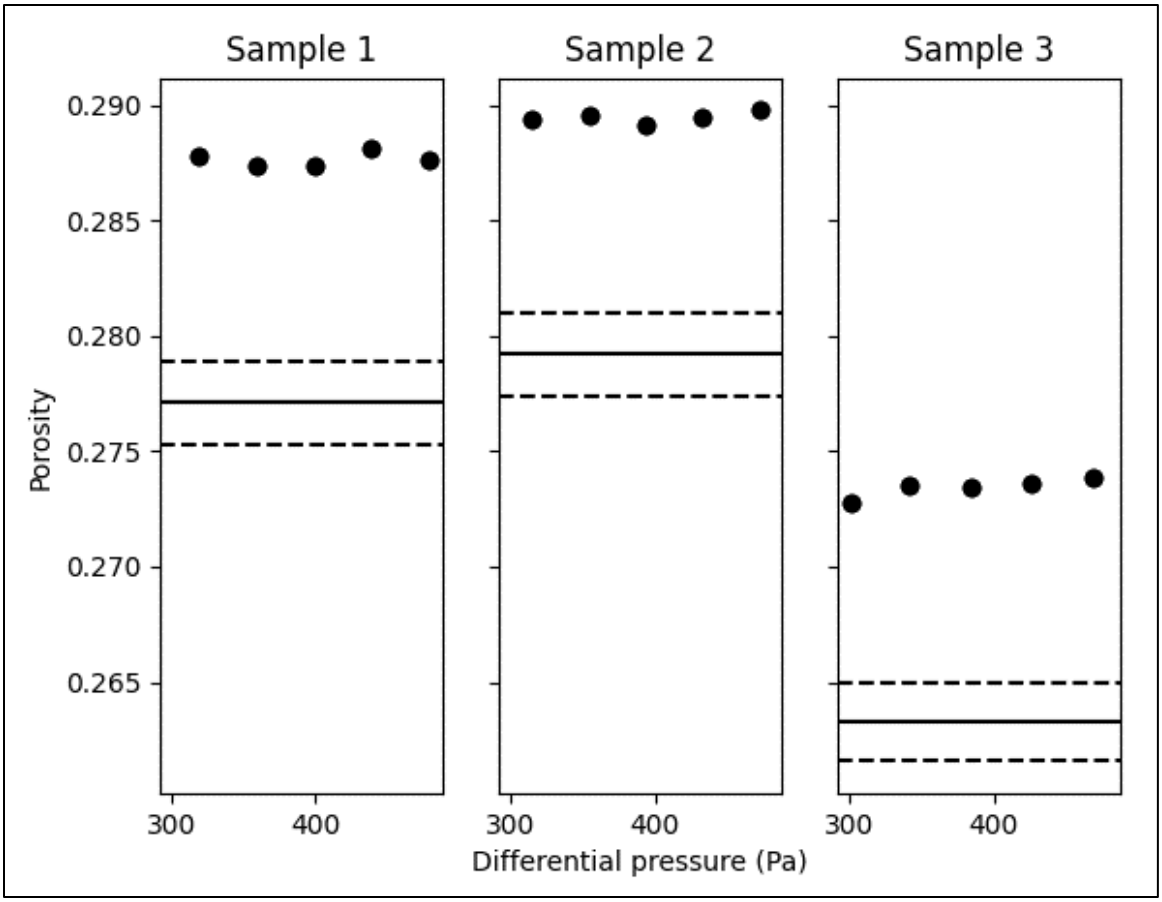

7.9 Filter Foam

Polyethylene filter foams of various pore sizes were used as porous samples in the porosimeter. Pore sizes of 10 ppi, 20 ppi, and 30 ppi were used. As the density of the solid material was not well known, water displacement measurements could be used to estimate the solid volume of the filter foam samples, with care being taken to fully saturate each sample. Measurement results are shown in Figures 22 to 24.

Porosimeter measurements of the filter foam showed good agreement with expected values of porosity, while showing a negative bias in all measurements. This differs from measurements taken on all other sample types, with measurements being less than the expected porosity and outside the uncertainty range. The negative bias may be a consequence of underestimating solid volumes (overestimating porosities) from water displacement measurements due to partial water saturation.

Figure 22. Porosimeter measurements of 10 pores per inch (ppi) polyether filter foam. The *solid lines* indicate expected porosity based on volume measurement, and the *dashed lines* indicate the expected range of uncertainty.

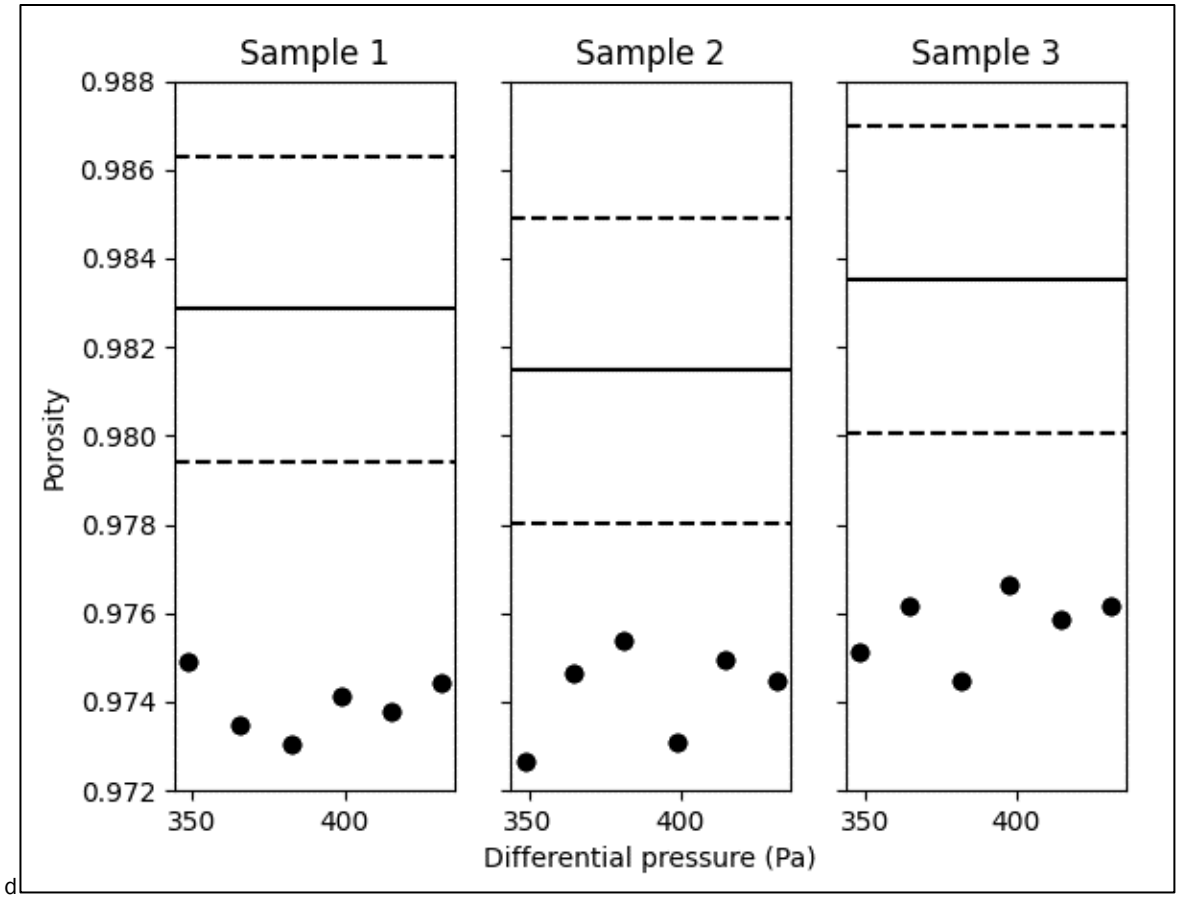

d

Figure 23. Porosimeter measurements of 20 ppi polyether filter foam. The *solid lines* indicate expected porosity based on volume measurement and the *dashed lines* indicate the expected range of uncertainty.

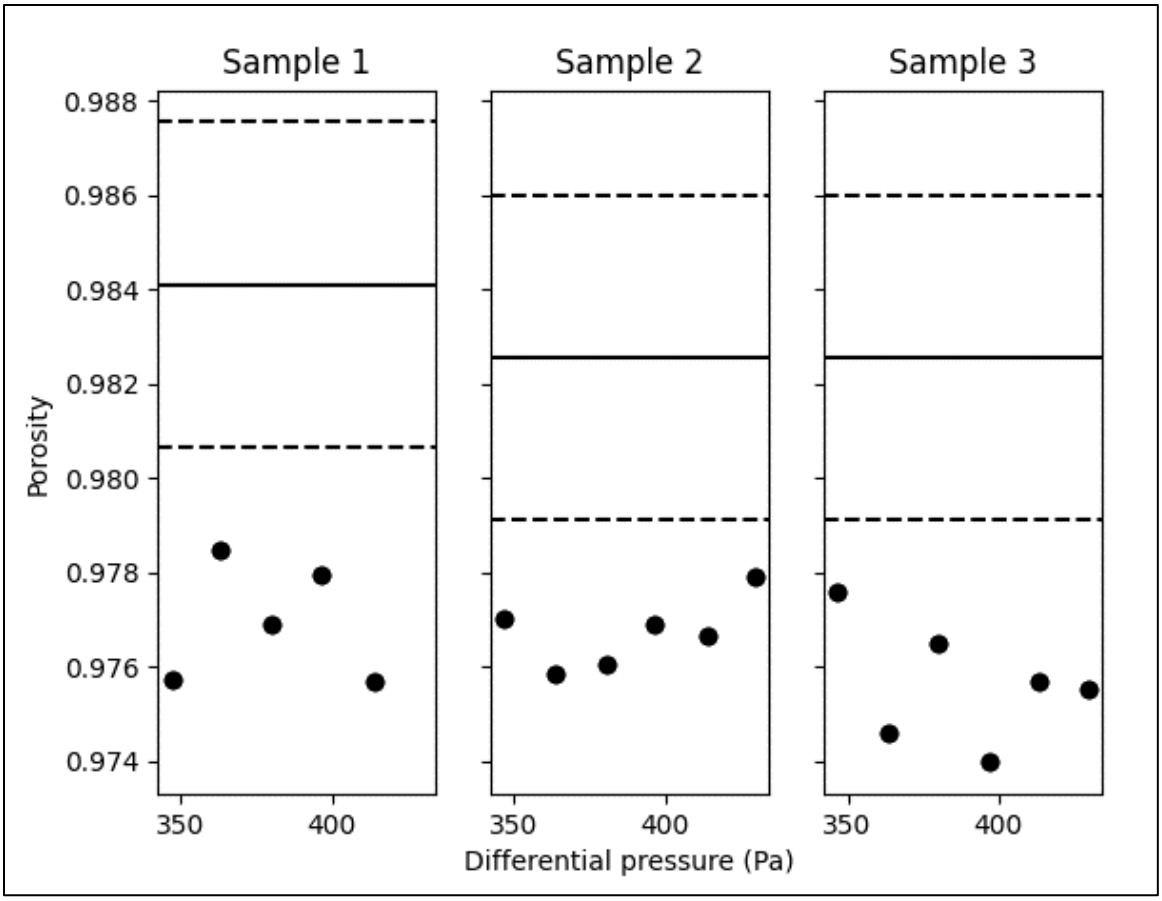

Figure 24. Porosimeter measurements of 30 ppi polyether filter foam. The *solid lines* indicate expected porosity based on volume measurement and the *dashed lines* indicate the expected range of uncertainty.

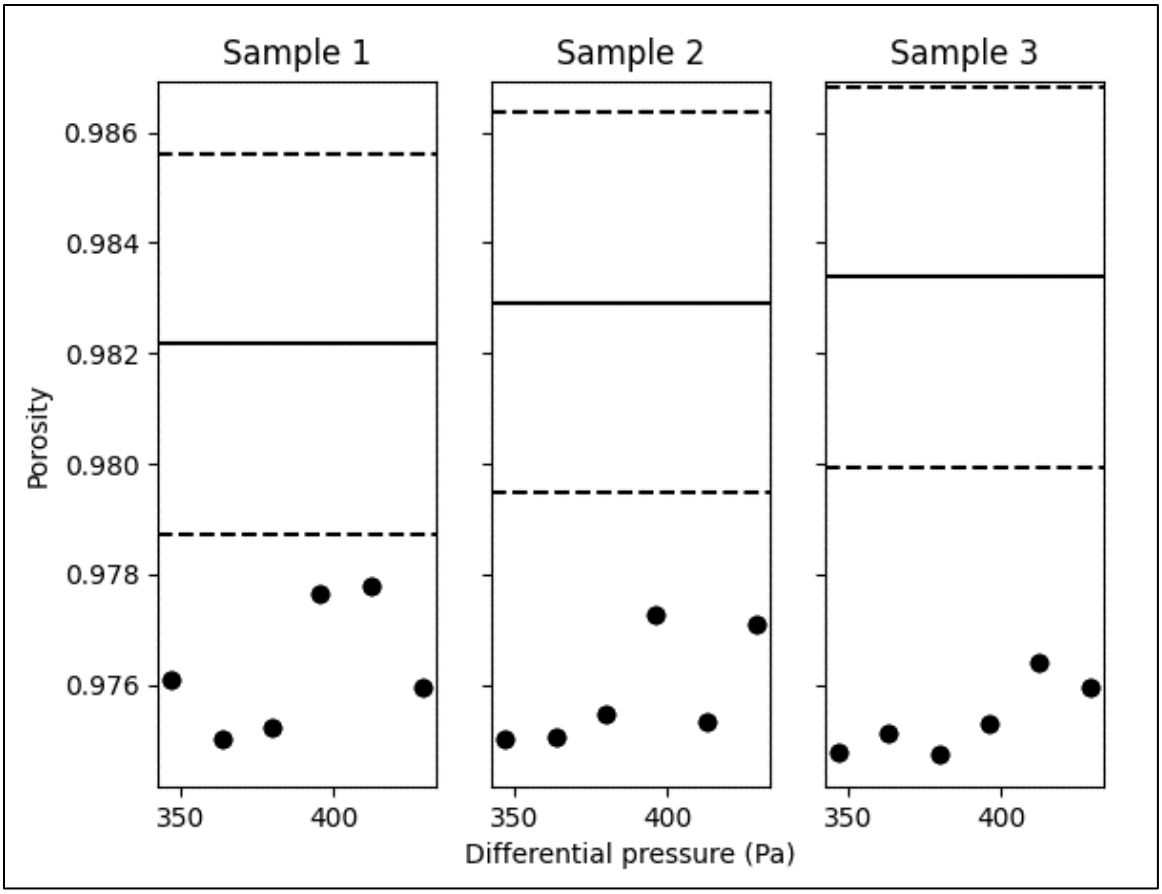

8 Discussion

After analysis, most initial measured values (before adjusting the residual volume based on the aluminum cylinder measurements) exceeded the range of uncertainty in expected porosity. This error could be due to a number of possibilities. Inaccuracy in material density and water displacement measurement errors are factors which could result in a bias for the expected value of porosity, thus resulting in an inaccurate uncertainty range. Error in the calibration (or simply a change in effective residual volume due to wear on the apparatus) could also lead to errors in the measurement values exceeding the uncertainty range for expected porosity. Calibration error was most likely based on the measurements taken as they showed a positive bias with the exception of the filter foam measurements, which suggests the effective residual volume was larger than previously measured. The filter foam was hypothesized to not show this bias as it was likely not fully saturated with water when taking volume measurements (this was clearly observed in foams with higher pore counts not included in this report). The adjusted residual volume was then used to adjust the measured porosity values as seen in Table 5.

After adjusting measurements to the updated effective residual volume, error was mostly decreased. The only exception to this decrease was the filter foam, which is expected to have errors in expected porosity as previously described. In the case of the solid aluminum cylinders and ball bearings, the adjusted average error was less than the expected uncertainties for those measurements. The glass beads adjusted average error exceeded the expected uncertainty on average; however, it was still small being less than 1%. The sintered plastic had large errors even after adjustment, likely due to the wide range in density that HDPE can have. Additionally, all spherical granular media (ball bearings and glass beads) have adjusted porosities similar to previous measurements taken on random packed spherical media which resulted in a range of 0.36 to 0.42 for porosity values (Dung et al. 2019).

Table 5. Measured porosities and errors before and after adjusting effective residual volume.

Material	Average Measured Porosity	Average Percent Error	Adjusted Measured Porosity	Adjusted Average Percent Error	Expected Uncertainty Percent
0.25 Solid Aluminum	0.253	1.26	0.250	0.166	0.75
0.50 Solid Aluminum	0.503	0.704	0.500	0.0855	0.75
0.75 Solid Aluminum	0.753	0.397	0.750	0.121	0.75
1/8 in. Ball Bearings	0.379	1.14	0.375	0.288	0.45
5/32 in. Ball Bearings	0.382	1.23	0.378	0.180	0.45
3/16 in. Ball Bearings	0.395	1.15	0.390	0.133	0.40
Glass Beads	0.390	1.86	0.386	0.744	0.45
10 ppi Filter Foam	0.978	0.452	0.975	0.813	0.35
20 ppi Filter Foam	0.980	0.321	0.977	0.674	0.35
30 ppi Filter Foam	0.982	0.135	0.976	0.709	0.35
200 µm Sintered Plastic	0.600	1.80	0.597	1.24	0.40
300 µm Sintered Plastic	0.540	2.56	0.536	1.93	0.45
400 µm Sintered Plastic	0.540	2.45	0.536	1.82	0.45
500 µm Sintered Plastic	0.287	5.18	0.283	3.78	0.65

9 Conclusion

The porosimeter described in this report is able to measure porosity with an average relative error less than 1%. The system was additionally designed and prototyped to meet physical and operational requirements for cold room testing. The system produced is in good agreement with the original design described by Champoux et al. (1991).

Measurements taken with the system showed high accuracy when compared to expected porosities for samples with well-known properties. Measurements on aluminum cylinders, ball bearings, and glass beads have average relative errors of less than 1%. Measurements on sintered HDPE plastic have greater inaccuracies due to the material's wide range of density, which affects the expected porosity obtained by a mass-density procedure. Measurements on filter foam have high accuracy, however, estimates of expected porosity by imbibition of water may be inaccurate due to partial saturation.

Initially, porosity measurements did not meet the accuracy expected by the uncertainty analysis for all measured samples. Adjusting the effective residual volume extends the measurement procedure of Champoux et al. (1991), and can bring the relative error within the bounds expected by an uncertainty analysis, as seen in the cases of the aluminum cylinders and the ball bearings. Because only one sample type with precisely measured geometry was used as a comparison to porosity, more samples of well-known porosity (measured geometrically or through use of indirect measurements such as microcomputed x-ray tomography) would need to be measured to determine the system's ability to meet the accuracy described by uncertainty analysis. Additionally, because an adjustment in the effective residual volume needed to be made after analyzing measurements, it is expected that the system can be recalibrated, or further analysis performed, to provide a higher accuracy.

While the porosimeter can measure porosity with high accuracy, many improvements could be made in the future. Further analysis on the apparent bias in measurements of glass beads, filter foams, and sintered plastic can be investigated. The test section can be designed with a faster clamping or lifting mechanism and a motor-driven micrometer to improve the efficiency of taking measurements. Further analysis on thermal effects on the apparatus, insulating the test section, and dynamic

measurements of air temperature within the test section are suggested. A thermal analysis would determine how close the measurement process matches isothermal conditions, and allow for adjustments to be made accordingly. The closer isothermal conditions are maintained, the lower is uncertainty for differential pressure.

Bibliography

Beranek, L. L. 1942. "Acoustic Impedance of Porous Materials." *Journal of the Acoustical Society of America* 13 (3): 248–260. https://doi.org/10.1121/1.1916172.

Champoux, Y., M. R. Stinson, and G. A. Daigle. 1991. "Air-Based System for the Measurement of Porosity." *Journal of the Acoustical Society of America* 89 (2): 910–916. https://doi.org/10.1121/1.1894653.

Dullien, F. A. 1979. *Porous Media: Fluid Transport and Pore Structure*. New York: Academic Press. https://www.sciencedirect.com/book/9780122236501/porous-media.

Dung, V. V., R. Panneton, and R. Gagne. 2019. "Prediction of Effective Properties and Sound Absorption of Random Close Packing of Monodisperse Spherical Particles: Multiscale Approach." *Journal of the Acoustical Society of America* 145 (6): 3606–3624. https://doi.org/10.1121/1.5111753.

ISO/IEC (International Organization for Standardization/International Electrotechnical Commission). 2008. *Uncertainty of Measurement—Part 3: Guide to the Expression of Uncertainty in Measurements (GUM:1995)*. Guide 98-3:2008(E). Geneva, Switzerland: International Organization for Standardization, International Electrotechnical Commission. https://www.iso.org/standard/50461.html.

Leclaire, P., O. Umnova, K. Horoshenkov, and L. Maillet. 2003. "Porosity Measurement by Comparison of Air Volumes." *Review of Scientific Instruments* 74 (3): 1366–1370. https://doi.org/10.1063/1.1542666.

Papoulis, A. 1991. *Probability, Random Variables, and Stochastic Processes*, 3rd ed. Chicago, IL: McGraw Hill.

Parker Hannifin Corporation. 2021. *Parker O-Ring Handbook*. ORD 5700. Cleveland, OH: Parker Hannifin Corporation. https://www.parker.com/content/dam/Parker-com/Literature/O-Ring-Division-Literature/ORD-5700.pdf.

Pompoli, F., P. Bonfiglio, K. V. Horoshenkov, A. Khan, L. Jaouen, F.-X. Bécot, F. Sgard, et al. 2017. "How Reproducible is the Acoustical Characterization of Porous Media?" *Journal of the Acoustical Society of America* 141 (2): 945–955. https://doi.org/10.1121/1.4976087.

Salissou, Y., and R. Panneton. 2007. "Pressure/Mass Method to Measure Open Porosity of Porous Solids." *Journal of Applied Physics* 101 (124913): 1–7. http://dx.doi.org/10.1063/1.2749486.

Abbreviations

CRREL	Cold Regions Research and Engineering Laboratory
ERDC	Engineer research and Development Center
FS	Full-scale
HS	Heat sink
ISO/IEC	International Organization for Standardization/ International Electrotechnical Commission
MH	Micrometer head
NPT	National Pipe Taper
ppi	Pores per inch
PT	Differential pressure transducer
RC	Reference chamber
WC	Water column

REPORT DOCUMENTATION PAGE

1. REPORT DATE	2. REPORT TYPE	3. DATES COVERED	
June 2024	Final Special Report (SR)	START DATE FY21	END DATE FY23

4. TITLE AND SUBTITLE

Porosity Measurement Device Design and Analysis

5a. CONTRACT NUMBER	5b. GRANT NUMBER	5c. PROGRAM ELEMENT
		601102A
5d. PROJECT NUMBER	**5e. TASK NUMBER**	**5f. WORK UNIT NUMBER**
AB2		

6. AUTHOR(S)

Cody M. Best, Carl R. Hart, and Christopher J. Donnelly

7. PERFORMING ORGANIZATION NAME(S) AND ADDRESS(ES)

US Army Engineer Research and Development Center (ERDC)
Cold Regions Research and Engineering Laboratory (CRREL)
72 Lyme Road
Hanover, NH 03755-1290

8. PERFORMING ORGANIZATION REPORT NUMBER

ERDC/CRREL SR-24-2

9. SPONSORING/MONITORING AGENCY NAME(S) AND ADDRESS(ES)	10. SPONSOR/MONITOR'S ACRONYM(S)	11. SPONSOR/MONITOR'S REPORT NUMBER(S)
US Army Corps of Engineers Washington, DC 20314-1000	USACE	

12. DISTRIBUTION/AVAILABILITY STATEMENT

Distribution Statement A. Approved for public release: distribution is unlimited.

13. SUPPLEMENTARY NOTES

14. ABSTRACT

Porosity measurements are necessary to fully characterize the acoustic properties of a porous material. Many methods exist to measure porosity with various limitations. This report details a system based on previous work to limit environmental effects on measurements.

15. SUBJECT TERMS

Porosity–Measurement; Porous materials–Acoustic properties; Scientific apparatus and instruments; Science–Methodology

16. SECURITY CLASSIFICATION OF:			17. LIMITATION OF ABSTRACT	18. NUMBER OF PAGES
a. REPORT	b. ABSTRACT	C. THIS PAGE		
Unclassified	Unclassified	Unclassified	SAR	57

19a. NAME OF RESPONSIBLE PERSON	19b. TELEPHONE NUMBER (include area code)
Carl R. Hart	(603) 646-4422